

Distinguishing between inflationary models from CMB

Shinji Tsujikawa

*Department of Physics, Faculty of Science, Tokyo University of Science, 1-3, Kagurazaka, Shinjuku-ku, Tokyo 162-8601, Japan, *E-mail: shinji@rs.kagu.tus.ac.jp*

.....

In this paper, inflationary cosmology is reviewed, paying particular attention to its observational signatures associated with large-scale density perturbations generated from quantum fluctuations. In the most general scalar-tensor theories with second-order equations of motion, we derive the scalar spectral index n_s , the tensor-to-scalar ratio r , and the nonlinear estimator f_{NL} of primordial non-Gaussianities to confront models with observations of Cosmic Microwave Background (CMB) temperature anisotropies. Our analysis includes models such as potential-driven slow-roll inflation, k-inflation, Starobinsky inflation, and Higgs inflation with non-minimal/derivative/Galileon couplings. We constrain a host of inflationary models by using the Planck data combined with other measurements to find models most favored observationally in the current literature. We also study anisotropic inflation based on a scalar coupling with a vector (or, two-form) field and discuss its observational signatures appearing in the two-point and three-point correlation functions of scalar and tensor perturbations.

1. Introduction

The inflationary paradigm was first proposed in the early 1980s to address the horizon, flatness, and monopole problems that plagued Big Bang cosmology [1, 2]. Moreover, inflation provides a causal mechanism for the generation of large-scale density perturbations from the quantum fluctuation of a scalar field (inflaton). In its simplest form the resulting power spectra of scalar and tensor perturbations are nearly scale-invariant and Gaussian [3]. This prediction showed good agreement with the temperature anisotropies of CMB measured by the Cosmic Background Explorer (COBE) [4] and the Wilkinson Microwave Anisotropy Probe (WMAP) [5]. In March 2013 the Planck team [6] released more accurate CMB data up to the multipoles $\ell \sim 2500$. With these new data it is now possible to discriminate between a host of inflationary models.

The first model of inflation, proposed by Starobinsky [1], is based on a conformal anomaly in quantum gravity. The Lagrangian density $f(R) = R + R^2/(6M^2)$, where R is a Ricci scalar and M is a mass scale of the order of 10^{13} GeV, can lead to a sufficient amount of inflation with a successful reheating [7]. Moreover, the Starobinsky model is favored from the 1-st year Planck observations [6]. The “old inflation” [2], which is based on the theory of supercooling during the cosmological phase transition, turned out to be unviable, because the Universe becomes inhomogeneous as a result of the bubble collision after inflation. The revised version dubbed “new inflation” [8, 9], where the second-order transition to true vacuum is responsible for cosmic acceleration, is plagued by a fine-tuning problem for spending enough time in false vacuum. However, these pioneering ideas opened up a new paradigm for the construction

of workable inflationary models based on theories beyond the Standard Model of particle physics (see e.g., Refs. [10–13]).

Most of the inflationary models, including chaotic inflation [14], are based on a slow-rolling scalar field with a sufficiently flat potential. One can discriminate between a host of inflaton potentials by comparing theoretical predictions of the scalar spectral index n_s and the tensor-to-scalar ratio r with the CMB temperature anisotropies (see, e.g., [15–18]). The Planck data, combined with the WMAP large-angle polarization (WP) measurement, placed the bounds $n_s = 0.9603 \pm 0.0073$ (68 % CL) and $r < 0.11$ (95 % CL) for the pivot wavenumber $k_0 = 0.002 \text{ Mpc}^{-1}$ [19]. Based on the paper [20], we review the observational bounds on potential-driven slow-roll inflation constrained from the joint data analysis of Planck [6], WP [21], Baryon Acoustic Oscillations (BAO) [22], and high- ℓ [23]¹

Besides slow-roll inflation, there is another class of models, called k-inflation models [24], in which the non-linear field kinetic energy plays a crucial role in driving cosmic acceleration. Since the scalar propagation speed c_s in k-inflation is generally different from the speed of light [25], this can give rise to large non-Gaussianities of primordial perturbations for the equilateral shape in the regime $c_s^2 \ll 1$ [26, 27]. Using the recent Planck bound on the equilateral non-linear parameter $f_{\text{NL}}^{\text{equil}} = -42 \pm 75$ (68 % CL) [28], it is possible to put tight constraints on most of the k-inflationary models.

There are also other single-field inflationary scenarios constructed in the framework of extended theories of gravity, such as non-minimally coupled models [29, 30], Brans-Dicke theories [31], Galileons [32–35], field derivative couplings to gravity [36, 37], and running kinetic couplings [38, 39]. All of these models are covered in Horndeski’s most general scalar-tensor theories with second-order equations of motion [40, 41]. For single-field inflation based on the Horndeski theory, the two-point and three-point correlation functions of scalar and tensor perturbations have been computed in Refs. [42–46] (see also Refs. [47]). We shall first review these results and then apply them to concrete models of inflation.

The WMAP5 data indicated that there is an anomaly associated with the broken rotational invariance of the CMB power spectrum [48]. This statistical anisotropy is difficult to address in the context of single-field slow-roll inflation. The power spectrum of curvature perturbations with broken statistical isotropy involves an anisotropy parameter g_* . This parameter was constrained as $g_* = 0.29 \pm 0.031$ (68 % CL) from the WMAP5 data by including multipoles up to $\ell = 400$ [49]. With the WMAP9 data, the bound $-0.046 < g_* < 0.048$ (68 % CL) was derived in Ref. [50]. Recently, Kim and Komatsu obtained the bound $g_* = 0.002 \pm 0.016$ (68 % CL) from the Planck data by taking into account the beam correction and the Galactic foreground correction [51]. This result is consistent with the isotropic power spectrum, but there is still a possibility that anisotropy of the order $|g_*| \sim 0.01$ remains.

For the models in which the inflaton field ϕ has a coupling to a vector kinetic term $F_{\mu\nu}F^{\mu\nu}$, an anisotropic hair can survive during inflation for a suitable choice of coupling $f^2(\phi)$ [52, 53]. In this case, it is possible to explain the anisotropic power spectrum compatible with the broken rotational invariance of the CMB perturbations [54, 55]. The same property also holds for the two-form field models in which the inflaton couples to the kinetic term $H_{\mu\nu\lambda}H^{\mu\nu\lambda}$ [56], but the types of anisotropies are different from each other. Moreover, these two anisotropic

¹Our review does not reflect constraints derived from the BICEPS2 data for the B-mode polarization, released in March 2014.

inflationary models can give rise to a detectable level of primordial non-Gaussianities [56–59]. We shall review the general properties of anisotropic inflation and discuss their observational signatures.

This review is organized as follows. In Sec. 2 we derive the two-point and three-point correlation functions of curvature perturbations and the resulting CMB observables in the Horndeski theory. In Sec. 3 we study observational constraints on potential-driven slow-roll inflation in the light of the Planck data. In Sec. 4 we distinguish between a host of single-field inflationary models that belong to the framework of the Horndeski theory. In Sec. 5 we discuss the current status of anisotropic inflation paying particular attention to their observational signatures. Sec. 6 is devoted to the conclusion.

2. Inflationary power spectra and non-Gaussianities in the most general scalar-tensor theories

For generality we start with the action of the most general scalar-tensor theories with second-order equations of motion [40–42]

$$S = \int d^4x \sqrt{-g} \left[\frac{M_{\text{pl}}^2}{2} R + P(\phi, X) - G_3(\phi, X) \square\phi + L_4 + L_5 \right], \quad (1)$$

where g is a determinant of the metric tensor $g_{\mu\nu}$, M_{pl} is the reduced Planck mass, R is the Ricci scalar, and

$$L_4 = G_4(\phi, X)R + G_{4,X}(\phi, X) [(\square\phi)^2 - \phi^{;\mu\nu}\phi_{;\mu\nu}], \quad (2)$$

$$L_5 = G_5(\phi, X)G_{\mu\nu}\phi^{;\mu\nu} - \frac{1}{6}G_{5,X}(\phi, X)[(\square\phi)^3 - 3(\square\phi)\phi_{;\mu\nu}\phi^{;\mu\nu} + 2\phi_{;\mu\nu}\phi^{;\mu\lambda}\phi^{;\nu}_{;\lambda}]. \quad (3)$$

Here, a semicolon represents a covariant derivative, P and G_i ($i = 3, 4, 5$) are functions in terms of ϕ and $X \equiv -\partial^\mu\phi\partial_\mu\phi/2$, and $G_{\mu\nu} = R_{\mu\nu} - g_{\mu\nu}R/2$ is the Einstein tensor ($R_{\mu\nu}$ is the Ricci tensor). For the partial derivatives with respect to ϕ and X , we use the notation $G_{i,\phi} \equiv \partial G_i/\partial\phi$ and $G_{i,X} \equiv \partial G_i/\partial X$.

On the flat Friedmann-Lemaître-Robertson-Walker (FLRW) background described by the line element $ds^2 = -dt^2 + a^2(t)\delta_{ij}dx^i dx^j$, the Friedmann equation and the scalar-field equation of motion are given, respectively, by [42–44]

$$\begin{aligned} 3M_{\text{pl}}^2 H^2 F &= P_{,X}\dot{\phi}^2 - P - (G_{3,\phi} - 12H^2 G_{4,X} + 9H^2 G_{5,\phi})\dot{\phi}^2 - 6HG_{4,\phi}\dot{\phi} \\ &- (6G_{4,\phi X} - 3G_{3,X} - 5G_{5,X}H^2)H\dot{\phi}^3 - 3(G_{5,\phi X} - 2G_{4,XX})H^2\dot{\phi}^4 + H^3 G_{5,XX}\dot{\phi}^5, \quad (4) \\ \frac{1}{a^3} \frac{d}{dt} (a^3 J) &= P_\phi, \quad (5) \end{aligned}$$

where $H = \dot{a}/a$ is the Hubble parameter (a dot represents a derivative with respect to t), $F = 1 + 2G_4/M_{\text{pl}}^2$, and

$$\begin{aligned} J &\equiv \dot{\phi}P_{,X} + 6HXG_{3,X} - 2\dot{\phi}G_{3,\phi} + 6H^2\dot{\phi}(G_{4,X} + 2XG_{4,XX}) - 12HXG_{4,\phi X} \\ &+ 2H^3X(3G_{5,X} + 2XG_{5,XX}) - 6H^2\dot{\phi}(G_{5,\phi} + XG_{5,\phi X}), \quad (6) \end{aligned}$$

$$\begin{aligned} P_\phi &\equiv P_{,\phi} - 2X(G_{3,\phi\phi} + \ddot{\phi}G_{3,\phi X}) + 6(2H^2 + \dot{H})G_{4,\phi} + 6H(\dot{X} + 2HX)G_{4,\phi X} \\ &- 6H^2XG_{5,\phi\phi} + 2H^3X\dot{\phi}G_{5,\phi X}. \quad (7) \end{aligned}$$

Inflation can be realized in the regime where the slow-roll parameter $\epsilon \equiv -\dot{H}/H^2$ is much smaller than 1. On using Eqs. (4) and (5), it follows that

$$\epsilon = \delta_{PX} + 3\delta_{G3X} - 2\delta_{G3\phi} + 6\delta_{G4X} - \delta_{G4\phi} - 6\delta_{G5\phi} + 3\delta_{G5X} + 12\delta_{G4XX} + 2\delta_{G5XX} + O(\epsilon^2), \quad (8)$$

where the slow-variation parameters on the r.h.s. are defined by $\delta_{PX} = P_{,X}X/(M_{\text{pl}}^2 H^2 F)$, $\delta_{G3X} = G_{3,X}\dot{\phi}X/(M_{\text{pl}}^2 HF)$, $\delta_{G3\phi} = G_{3,\phi}X/(M_{\text{pl}}^2 H^2 F)$, $\delta_{G4X} = G_{4,X}X/(M_{\text{pl}}^2 F)$, $\delta_{G4\phi} = G_{4,\phi}\dot{\phi}/(M_{\text{pl}}^2 HF)$, $\delta_{G5\phi} = G_{5,\phi}X/(M_{\text{pl}}^2 F)$, $\delta_{G5X} = G_{5,X}H\dot{\phi}X/(M_{\text{pl}}^2 F)$, $\delta_{G4XX} = G_{4,XX}X^2/(M_{\text{pl}}^2 F)$, and $\delta_{G5XX} = G_{5,XX}H\dot{\phi}X^2/(M_{\text{pl}}^2 F)$.

The number of e-foldings is defined as $N(t) = \ln a(t_f)/a(t)$, where $a(t)$ and $a(t_f)$ are the scale factors at time t during inflation and at the end of inflation respectively. On using the relation $dN/dt = -H(t)$, it can also be expressed as

$$N(t) = - \int_{t_f}^t H(\tilde{t}) d\tilde{t}, \quad (9)$$

where t_f is known by the relation $\epsilon(t_f) = 1$. The number of e-foldings when the perturbations relevant to the CMB temperature anisotropies cross the Hubble radius is typically in the range $50 < N < 60$ [19, 60].

For the computations of the two-point and three-point correlation functions of scalar and tensor perturbations, we use the following perturbed ADM metric [61] on the flat FLRW background

$$ds^2 = -[(1 + \alpha)^2 - a^{-2}(t)e^{-2\psi}(\partial B)^2]dt^2 + 2\partial_i B dt dx^i + a^2(t)(e^{2\psi}\delta_{ij} + h_{ij})dx^i dx^j, \quad (10)$$

where α, B, ψ describe scalar metric perturbations, and h_{ij} is the tensor perturbation. The choice of the ADM metric is particularly convenient for the calculation of non-Gaussianities [62, 63]. Note that, at linear order in perturbations, the coefficient in front of dt^2 in Eq. (10) reduces to $-(1 + 2\alpha)$. We introduce the gauge-invariant curvature perturbation [64]

$$\zeta = \psi - \frac{H}{\dot{\phi}}\delta\phi, \quad (11)$$

where $\delta\phi$ is the perturbation in the field ϕ . We choose unitary gauge $\delta\phi = 0$ to fix the time component of a gauge-transformation vector ξ^μ . The scalar perturbation E , which appears in the metric (10) in the form $E_{,ij}$, is gauged away, so that the spatial component of ξ^μ is fixed (see Refs. [65, 66] for details of the cosmological perturbation theory).

Expanding the action (1) up to second order in perturbations, we can derive the equations of motion for linear perturbations. Variations of the second-order action with respect to α and B lead to the Hamiltonian and momentum constraints, respectively, by which α and B can be related to the curvature perturbation ζ . Then, the resulting second-order action of scalar perturbations reads [20, 42–44]

$$S_s^{(2)} = \int dt d^3x a^3 Q_s \left[\dot{\zeta}^2 - \frac{c_s^2}{a^2} (\partial\zeta)^2 \right]. \quad (12)$$

At leading order in slow-variation parameters we have

$$Q_s = M_{\text{pl}}^2 F q_s, \quad (13)$$

$$q_s \equiv \delta_{PX} + 2\delta_{PXX} + 6\delta_{G3X} + 6\delta_{G3XX} + 6\delta_{G4X} + 48\delta_{G4XX} + 24\delta_{G4XXX} \\ + 6\delta_{G5X} + 14\delta_{G5XX} + 4\delta_{G5XXX} - 2\delta_{G3\phi} - 6\delta_{G5\phi}, \quad (14)$$

$$\epsilon_s \equiv \frac{Q_s c_s^2}{M_{\text{pl}}^2 F} = \delta_{PX} + 4\delta_{G3X} + 6\delta_{G4X} + 20\delta_{G4XX} + 4\delta_{G5X} + 4\delta_{G5XX} - 2\delta_{G3\phi} - 6\delta_{G5\phi}, \quad (15)$$

where $\delta_{PXX} = X^2 P_{,XX}/(M_{\text{pl}}^2 H^2 F)$, $\delta_{G4XXX} = G_{4,XXX} X^3/(M_{\text{pl}}^2 F)$, and $\delta_{G5XXX} = G_{5,XXX} H \dot{\phi} X^3/(M_{\text{pl}}^2 F)$. From Eqs. (13) and (15), the scalar propagation speed c_s is given by

$$c_s^2 = \frac{\epsilon_s}{q_s}. \quad (16)$$

As we will see later, the tensor ghost is absent for $F > 0$. As long as $q_s > 0$ and $\epsilon_s > 0$, we can avoid the ghost and Laplacian instabilities of scalar perturbations.

We write the curvature perturbation in terms of Fourier components, as

$$\zeta(\tau, \mathbf{x}) = \frac{1}{(2\pi)^3} \int d^3 \mathbf{k} \hat{\zeta}(\tau, \mathbf{k}) e^{i\mathbf{k}\cdot\mathbf{x}}, \quad \hat{\zeta}(\tau, \mathbf{k}) = \zeta(\tau, \mathbf{k}) a(\mathbf{k}) + \zeta^*(\tau, -\mathbf{k}) a^\dagger(-\mathbf{k}), \quad (17)$$

where $\tau = \int a^{-1} dt$ is the conformal time, \mathbf{k} is a comoving wavenumber, and $a(\mathbf{k})$ and $a^\dagger(\mathbf{k})$ are the annihilation and creation operators, respectively, satisfying the commutation relations

$$[a(\mathbf{k}_1), a^\dagger(\mathbf{k}_2)] = (2\pi)^3 \delta^{(3)}(\mathbf{k}_1 - \mathbf{k}_2), \quad [a(\mathbf{k}_1), a(\mathbf{k}_2)] = [a^\dagger(\mathbf{k}_1), a^\dagger(\mathbf{k}_2)] = 0. \quad (18)$$

Since $\tau = -1/(aH)$ in the de Sitter background, the asymptotic past and future correspond to $\tau \rightarrow -\infty$ and $\tau \rightarrow -0$, respectively. Introducing a field $v = z\zeta$ with $z = a\sqrt{2Q_s}$ the kinetic term in the second-order action (12) can be rewritten as $\int d\tau d^3x v'^2/2$, where a prime represents a derivative with respect to τ . Hence v is a canonical field that should be quantized. In Fourier space the field v obeys the differential equation

$$v'' + \left(c_s^2 k^2 - \frac{z''}{z} \right) v = 0. \quad (19)$$

In the de Sitter background with a slow variation of the quantity Q_s , we have $z''/z \simeq 2/\tau^2$. In the asymptotic past ($k\tau \rightarrow -\infty$) we choose the Bunch-Davies vacuum characterized by the mode function $v = e^{-ic_s k\tau}/\sqrt{2c_s k}$. Then the solution of Eq. (19) reads

$$\zeta(\tau, k) = \frac{i H e^{-ic_s k\tau}}{2(c_s k)^{3/2} \sqrt{Q_s}} (1 + ic_s k\tau). \quad (20)$$

The two-point correlation function, some time after the Hubble radius crossing, is given by the vacuum expectation value $\langle 0 | \hat{\zeta}(\tau, \mathbf{k}_1) \hat{\zeta}(\tau, \mathbf{k}_2) | 0 \rangle$ at $\tau \approx 0$. We define the scalar power

spectrum $\mathcal{P}_\zeta(k_1)$, as

$$\langle 0|\hat{\zeta}(0, \mathbf{k}_1)\hat{\zeta}(0, \mathbf{k}_2)|0\rangle = (2\pi^2/k_1^3)\mathcal{P}_\zeta(k_1)(2\pi)^3\delta^{(3)}(\mathbf{k}_1 + \mathbf{k}_2). \quad (21)$$

On using the solution (20), the resulting power spectrum of ζ is

$$\mathcal{P}_\zeta = \frac{H^2}{8\pi^2 M_{\text{pl}}^2 \epsilon_s F c_s} \Big|_{c_s k = aH}, \quad (22)$$

which is evaluated at $c_s k = aH$ (because ζ is nearly frozen for $c_s k < aH$). The scalar spectral index reads

$$n_s - 1 \equiv \frac{d \ln \mathcal{P}_\zeta}{d \ln k} \Big|_{c_s k = aH} = -2\epsilon - \eta_s - \delta_F - s, \quad (23)$$

where

$$\eta_s \equiv \frac{\dot{\epsilon}_s}{H \epsilon_s}, \quad s \equiv \frac{\dot{c}_s}{H c_s}, \quad \delta_F \equiv \frac{\dot{F}}{H F}. \quad (24)$$

The running spectral index is defined by $\alpha_s \equiv dn_s/d \ln k|_{c_s k = aH}$, which is of the order of ϵ^2 from Eq. (23).

We can decompose the transverse and traceless tensor perturbations into two independent polarization modes, as $h_{ij} = h_+ e_{ij}^+ + h_\times e_{ij}^\times$, where e_{ij}^λ (where $\lambda = +, \times$) satisfy the relations $e_{ij}^+(\mathbf{k})e_{ij}^+(-\mathbf{k})^* = 2$, $e_{ij}^\times(\mathbf{k})e_{ij}^\times(-\mathbf{k})^* = 2$, and $e_{ij}^+(\mathbf{k})e_{ij}^\times(-\mathbf{k})^* = 0$. The second-order action for h_{ij} reads [42–44]

$$S_t^{(2)} = \sum_{\lambda=+, \times} \int dt d^3x a^3 Q_t \left[\dot{h}_\lambda^2 - \frac{c_t^2}{a^2} (\partial h_\lambda)^2 \right], \quad (25)$$

where

$$Q_t = \frac{1}{4} M_{\text{pl}}^2 F (1 - 4\delta_{G4X} - 2\delta_{G5X} + 2\delta_{G5\phi}), \quad (26)$$

$$c_t^2 = 1 + 4\delta_{G4X} + 2\delta_{G5X} - 4\delta_{G5\phi} + O(\epsilon^2). \quad (27)$$

Following a similar procedure to that for scalar perturbations, we obtain the tensor power spectrum

$$\mathcal{P}_h = \frac{H^2}{2\pi^2 Q_t c_t^3} \Big|_{c_t k = aH} \simeq \frac{2H^2}{\pi^2 M_{\text{pl}}^2 F} \Big|_{k = aH}, \quad (28)$$

where, in the second approximate equality, we have taken leading-order terms of Eqs. (26) and (27).

At the epoch when both ζ and h_λ become nearly constant during inflation, the tensor-to-scalar ratio can be evaluated as

$$r = \frac{\mathcal{P}_h}{\mathcal{P}_\zeta} \simeq 16c_s \epsilon_s. \quad (29)$$

Then the tensor spectral index is given by

$$n_t \equiv \frac{d \ln \mathcal{P}_h}{d \ln k} \Big|_{k = aH} = -2\epsilon - \delta_F. \quad (30)$$

The tensor running $\alpha_t \equiv dn_t/d \ln k|_{k = aH}$ is of the order of ϵ^2 . On using Eqs. (8) and (15) as well as the relation $\delta_F \simeq 2G_{G4\phi} + O(\epsilon^2)$, we obtain the consistency relation

$$r = -8c_s (n_t - 2\delta_{G3X} - 16\delta_{G4XX} - 2\delta_{G5X} - 4\delta_{G5XX}). \quad (31)$$

The three-point correlation function of curvature perturbations associated with scalar non-Gaussianities has been computed in Refs. [43, 44]. The bispectrum A_ζ is defined by

$$\langle \zeta(\mathbf{k}_1)\zeta(\mathbf{k}_2)\zeta(\mathbf{k}_3) \rangle = (2\pi)^7 \delta^{(3)}(\mathbf{k}_1 + \mathbf{k}_2 + \mathbf{k}_3) (\mathcal{P}_\zeta)^2 \frac{A_\zeta(k_1, k_2, k_3)}{\prod_{i=1}^3 k_i^3}. \quad (32)$$

The non-linear estimator, $f_{\text{NL}} = (10/3)A_\zeta / \sum_{i=1}^3 k_i^3$, is commonly used to characterize the level of non-Gaussianities [62, 67, 68]. In Refs. [43, 44] the leading-order bispectrum was derived on the de Sitter background. Reference [69] evaluated the three-point correlation function by taking into account all possible slow-variation corrections to the leading-order term (along the lines of Ref. [27]). Under the slow-variation approximation where each term appearing on the r.h.s. of Eq. (8) is much smaller than 1, the non-linear estimator in the squeezed limit ($k_3 \rightarrow 0$, $k_1 \rightarrow k_2$) reads [69]

$$f_{\text{NL}}^{\text{local}} = \frac{5}{12}(1 - n_s), \quad (33)$$

which is consistent with the result of Refs. [62, 70]. Since $f_{\text{NL}}^{\text{local}} = O(\epsilon)$, the Planck bound $f_{\text{NL}}^{\text{local}} = 2.7 \pm 5.8$ (68 % CL) [28] is satisfied for all the slow-variation single-field models based on the Horndeski theory. There are some non-slow roll models in which the non-Gaussianity consistency relation (33) is violated [71], but we do not study such specific cases.

In the limit of the equilateral triangle ($k_1 = k_2 = k_3$), the leading-order non-linear parameter is given by [69]

$$f_{\text{NL}}^{\text{equil}} = \frac{85}{324} \left(1 - \frac{1}{c_s^2}\right) - \frac{10}{81} \frac{\lambda}{\Sigma} + \frac{20}{81\epsilon_s} [\delta_{G3X} + \delta_{G3XX} + 4(3\delta_{G4XX} + 2\delta_{G4XXX}) + \delta_{G5X} + 5\delta_{G5XX} + 2\delta_{G5XXX}] + \frac{65}{162c_s^2\epsilon_s} (\delta_{G3X} + 6\delta_{G4XX} + \delta_{G5X} + \delta_{G5XX}), \quad (34)$$

where

$$\begin{aligned} \lambda &= \frac{F^2}{3} [3X^2 P_{,XX} + 2X^3 P_{,XXX} + 3H\dot{\phi}(XG_{3,X} + 5X^2 G_{3,XX} + 2X^3 G_{3,XXX}) \\ &\quad - 2(2X^2 G_{3,\phi X} + X^3 G_{3,\phi XX}) + 6H^2(9X^2 G_{4,XX} + 16X^3 G_{4,XXX} + 4X^4 G_{4,XXXX}) \\ &\quad - 3H\dot{\phi}(3XG_{4,\phi X} + 12X^2 G_{4,\phi XX} + 4X^3 G_{4,\phi XXX}) + H^3\dot{\phi}(3XG_{5,X} + 27X^2 G_{5,XX} \\ &\quad + 24X^3 G_{5,XXX} + 4X^4 G_{5,XXXX}) - 6H^2(6X^2 G_{5,\phi X} + 9X^3 G_{5,\phi XX} + 2X^4 G_{5,\phi XXX})], \\ \Sigma &= \frac{Q_s}{4M_{\text{pl}}^4} [2M_{\text{pl}}^2 H F - 2X\dot{\phi}G_{3,X} - 16H(XG_{4,X} + X^2 G_{4,XX}) + 2\dot{\phi}(G_{4,\phi} + 2XG_{4,\phi X}) \\ &\quad - 2H^2\dot{\phi}(5XG_{5,X} + 2X^2 G_{5,XX}) + 4HX(3G_{5,\phi} + 2XG_{5,\phi X})]^2. \end{aligned} \quad (35)$$

For the models in which c_s^2 is much smaller than 1, the nonlinear estimator $|f_{\text{NL}}^{\text{equil}}|$ can be much larger than 1. The Planck team derived the bound $f_{\text{NL}}^{\text{equil}} = -42 \pm 75$ (68 % CL) [28] by using three optimal bispectrum estimators. The primordial non-Gaussianities provide additional constraints on the models to those derived from n_s and r .

3. Planck constraints on potential-driven slow-roll inflation

Let us first study observational constraints on standard slow-roll inflation characterized by the functions

$$P(\phi, X) = X - V(\phi), \quad G_3 = 0, \quad G_4 = 0, \quad G_5 = 0, \quad (36)$$

where $V(\phi)$ is the inflaton potential. Under the slow-roll approximations $\dot{\phi}^2/2 \ll V$ and $|\ddot{\phi}| \ll |3H\dot{\phi}|$, Eqs. (4) and (5) reduce to $3M_{\text{pl}}^2 H^2 \simeq V$ and $3H\dot{\phi} \simeq -V_{,\phi}$ respectively. Then the number of e-foldings (9) can be expressed as

$$N \simeq \frac{1}{M_{\text{pl}}^2} \int_{\phi_f}^{\phi} \frac{V}{V_{,\phi}} d\tilde{\phi}, \quad (37)$$

where ϕ_f is the field value at the end of inflation known by the condition $\epsilon(\phi_f) = 1$.

The slow-roll parameter ϵ is equivalent to $\epsilon_s = \dot{\phi}^2/(2M_{\text{pl}}^2 H^2)$. Under the slow-roll approximation it follows that $\epsilon_s \simeq \epsilon_V$ and $\eta_s \simeq 4\epsilon_V - 2\eta_V$, where

$$\epsilon_V \equiv \frac{M_{\text{pl}}^2}{2} \left(\frac{V_{,\phi}}{V} \right)^2, \quad \eta_V \equiv \frac{M_{\text{pl}}^2 V_{,\phi\phi}}{V}. \quad (38)$$

Using the fact that $c_s^2 = 1$ and $F = 1$, the observables (23), (29), and (30) reduce to

$$n_s = 1 - 6\epsilon_V + 2\eta_V, \quad r = -8n_t, \quad n_t = -2\epsilon_V. \quad (39)$$

For a given inflaton potential these observables can be expressed in terms of ϕ . The field value corresponding to $N = 50 \sim 60$ is known by Eq. (37).

For observational constraints on inflationary models based on the Planck data, we expand the scalar and tensor power spectra around a pivot wavenumber k_0 , as

$$\ln \mathcal{P}_\zeta(k) = \ln \mathcal{P}_\zeta(k_0) + [n_s(k_0) - 1]x + \alpha_s(k_0)x^2/2 + O(x^3), \quad (40)$$

$$\ln \mathcal{P}_h(k) = \ln \mathcal{P}_h(k_0) + n_t(k_0)x + \alpha_t(k_0)x^2/2 + O(x^3), \quad (41)$$

where $x = \ln(k/k_0)$. Since the likelihood results are insensitive to the choice of k_0 , we fix $k_0 = 0.05 \text{ Mpc}^{-1}$ as in Ref. [20]. Since the runnings $|\alpha_s(k_0)|$ and $|\alpha_t(k_0)|$ are of the order of ϵ^2 under the slow-roll approximation, we also set these values to 0. Using the consistency relation $r(k_0) = -8n_t(k_0)$, the three inflationary observables $\mathcal{P}_\zeta(k_0)$, $n_s(k_0)$, and $r(k_0)$ are varied in the likelihood analysis. We also assume the flat Λ CDM model with $N_{\text{eff}} = 3.046$ relativistic degrees of freedom [72] and employ the standard Big Bang nucleosynthesis consistency relation [73]. In addition to the Planck data [19], we also use the data of WP [21], BAO [22], and high- ℓ [23].

In Fig. 1 we plot the 68% and 95% CL boundaries in the (n_s, r) plane constrained by the joint data analyses of Planck, WP, BAO, high- ℓ data (thick solid curves) and Planck, WP, BAO data (thick dotted curves). With the high- ℓ data, the scalar spectral index shifts toward smaller values and the tensor-to-scalar ratio gets slightly smaller. In what follows we place observational constraints on a number of representative inflaton potentials. For observational bounds on other potentials, we refer the reader to Ref. [18]. The Planck constraints on braneworld inflation [74] and non-commutative inflation [75] have been studied in Ref. [76] for several inflaton potentials discussed below, but we do not have any significant observational evidence that they are particularly favored over standard slow-roll inflation.

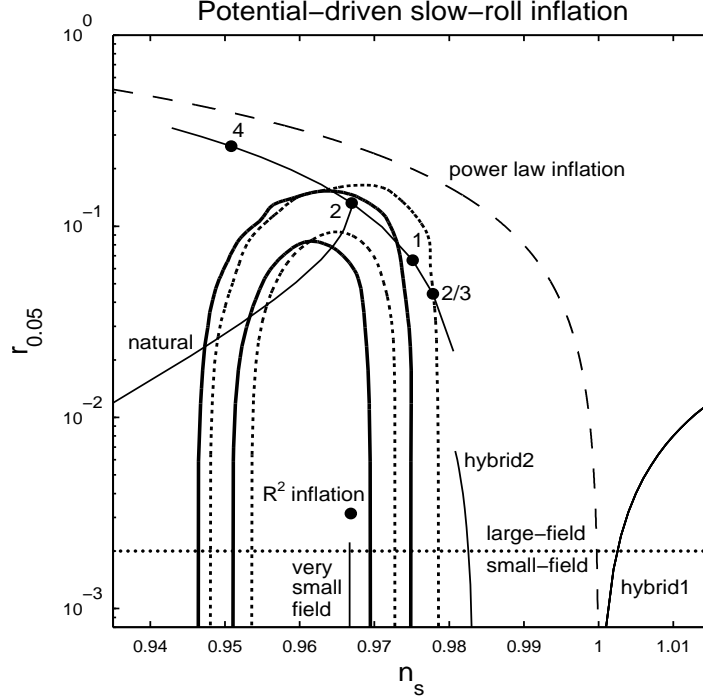


Fig. 1 Observational constraints on potential-driven slow-roll inflation in the (n_s, r) plane with $N = 60$ and $k_0 = 0.05 \text{ Mpc}^{-1}$. The thick solid and dotted curves correspond to the 68 % CL (inside) and 95 % CL (outside) boundaries derived by the joint data analysis of Planck+WP+BAO+high- ℓ and that of Planck+WP+BAO, respectively. We show the theoretical predictions for the models: (i) chaotic inflation with the potential $V(\phi) = \lambda_n \phi^n/n$ for general n (thin solid curve) and for $n = 4, 2, 1, 2/3$ (denoted by black circles), (ii) natural inflation with the potential $V(\phi) = \Lambda^4[1 + \cos(\phi/f)]$ for general f , (iii) hybrid inflation with the potentials $V(\phi) = \Lambda^4 + m^2 \phi^2/2$ (“hybrid1”) and $V(\phi) = \Lambda^4[1 + c \ln(\phi/\mu)]$ (“hybrid2”), (iv) very small-field inflation with the potential $V(\phi) = \Lambda^4(1 - e^{-\phi/M})$ in the regime $M < M_{\text{pl}}$, and (v) power-law inflation with the exponential potential $V(\phi) = V_0 e^{-\gamma \phi/M_{\text{pl}}}$. The dotted line ($r = 2 \times 10^{-3}$) corresponds to the boundary between “large-field” and “small-field” models. We also show the theoretical prediction of the Starobinsky model $f(R) = R + R^2/(6M^2)$ (shown as “ R^2 inflation” in the figure).

3.1. Chaotic inflation

Chaotic inflation is characterized by the potential [8]

$$V(\phi) = \lambda_n \phi^n/n, \quad (42)$$

where n and λ_n are positive constants. In this case the slow-roll parameters (38) reduce to $\epsilon_V = n^2 M_{\text{pl}}^2/(2\phi^2)$ and $\eta_V = n(n-1)M_{\text{pl}}^2/\phi^2$. From Eq. (37) we obtain the relation $\phi^2(N) \simeq 2n(N + n/4)M_{\text{pl}}^2$, where we used $\phi_f = nM_{\text{pl}}/\sqrt{2}$. The scalar spectral index and the tensor-to-scalar ratio read

$$n_s = 1 - \frac{2(n+2)}{4N+n}, \quad r = \frac{8n}{n+2}(1-n_s). \quad (43)$$

As we see in Fig. 1, the quartic potential ($n = 4$) is far outside the 95 % CL contour. For the quadratic potential ($n = 2$) we have $n_s = 0.967$ and $r = 0.132$ for $N = 60$, which is marginally inside the 95 % CL boundary constrained by the Planck+WP+BAO+high- ℓ data. For $N = 50$ the quadratic potential is outside the 95 % CL region.

The potentials with the powers $n = 1$ and $n = 2/3$ appear in the axion monodromy scenario [77, 78]. For $N = 60$, the linear potential is within the 95 % CL region constrained by the Planck+WP+BAO data, but it is outside the 95 % CL boundary by adding the high- ℓ data. For $N = 50$ the linear potential enters the joint 95 % CL region constrained by the Planck+WP+BAO+high- ℓ data due to the decrease of n_s . For $N = 60$ the potential with $n = 2/3$ is outside the joint 95 % CL boundary derived by the Planck+WP+BAO+high- ℓ data, but for $N = 50$ the model marginally lies within the 95 % CL contour.

The exponential potential $V(\phi) = V_0 e^{-\gamma\phi/M_{\text{pl}}}$ corresponds to the limit $n \rightarrow \infty$ in Eq. (43), which is characterized by the line $r = 8(1 - n_s)$. This model, which is shown as a dashed curve in Fig. 1, is excluded at more than 95 % CL.

3.2. Natural inflation

We proceed to natural inflation given by the potential [79]

$$V(\phi) = \Lambda^4 [1 + \cos(\phi/f)] , \quad (44)$$

where Λ and f are constants. From Eq. (37) the number of e-foldings can be estimated as $N \simeq \delta_f^{-1} \ln\{(2\epsilon_V + \delta_f)/[(2 + \delta_f)\epsilon_V]\}$, where $\delta_f = M_{\text{pl}}^2/f^2$. This is inverted to give

$$\epsilon_V \simeq \frac{\delta_f}{e^{N\delta_f}(2 + \delta_f) - 2} . \quad (45)$$

The slow-roll parameter η_V is related to ϵ_V via

$$\eta_V = \epsilon_V - \delta_f/2 . \quad (46)$$

For given values of N and f , we can evaluate $n_s = 1 - 4\epsilon_V - \delta_f$ and $r = 16\epsilon_V$ by using Eq. (45). In the limit that $f \rightarrow \infty$, inflation occurs in the regime where ϕ is close to the potential minimum ($\phi = \pi f$). Since $\epsilon_V \rightarrow 1/(2N + 1)$ and $\delta_f \rightarrow 0$ in this limit, we obtain $n_s = 1 - 4/(2N + 1)$ and $r = 16/(2N + 1)$, which correspond to the values of chaotic inflation with $n = 2$.

In Fig. 1, we plot the theoretical values of n_s and r for $N = 60$ as a function of f . For decreasing f , both n_s and r get smaller. From the joint analysis of the Planck+WP+BAO+high- ℓ data, the symmetry-breaking scale f is constrained as

$$5.1M_{\text{pl}} < f < 7.9M_{\text{pl}} \quad (68 \text{ \% CL}) , \quad (47)$$

whereas $f > 4.6M_{\text{pl}}$ at 95 % CL.

3.3. Hybrid inflation

Hybrid inflation involves two scalar fields: the inflaton ϕ and another symmetry-breaking field χ . During inflation the field χ is close to 0, in which regime the potential is approximately given by

$$V(\phi) \simeq \Lambda^4 + U(\phi) , \quad (48)$$

where Λ is a constant, and $U(\phi)$ depends on ϕ . Inflation ends due to a waterfall transition driven by the growth of χ . Linde's original hybrid model [80] corresponds to $U(\phi) = m^2\phi^2/2$.

Provided that the ratio $r_U \equiv U(\phi)/\Lambda^4$ is much smaller than 1, it follows that

$$n_s \simeq 1 + \frac{2m^2 M_{\text{pl}}^2}{\Lambda^4}, \quad r \simeq 8(n_s - 1)r_U. \quad (49)$$

Hence the scalar power spectrum is blue-tilted ($n_s > 1$). Under the condition $r_U < 0.1$, the tensor-to-scalar ratio is bounded as $r < 0.8(n_s - 1)$ (which is shown as a solid curve in Fig. 1 in the regime $n_s > 1$). The hybrid model with $U(\phi) = m^2\phi^2/2$ is far outside the 95 % CL region.

There is also a supersymmetric GUT model characterized by the potential $V(\phi) = \Lambda^4 + c\Lambda^4 \ln(\phi/\mu)$ with $c \ll 1$ [81]. In the regime where ϕ is much larger than the field value ϕ_c at the bifurcation point, the observables are given by $n_s \simeq 1 - (2 + 3c)/(2N)$ and $r \simeq 4c/N$, where we have used $N \simeq \phi^2/(2M_{\text{pl}}^2 c)$. Since the second derivative $V_{,\phi\phi}$ is negative, the spectrum is red-tilted. In Fig. 1 the theoretical curves are plotted for $0 < c < 0.1$ and $N = 60$. The model is outside the 95 % CL region constrained by the Planck+WP+BAO+high- ℓ data due to the large scalar spectral index.

3.4. Very small-field inflation

The tensor-to-scalar ratio is related to the variation of the field during inflation. In fact, we obtain the relation $(d\phi/dN)^2 \simeq M_{\text{pl}}^2 r/8$ from Eqs. (37)-(39). Provided that r is nearly constant during inflation, the field variation $\Delta\phi$ is approximately given by [82, 83]

$$\frac{\Delta\phi}{M_{\text{pl}}} \simeq \left(\frac{r}{2 \times 10^{-3}} \right)^{1/2} \left(\frac{N}{60} \right). \quad (50)$$

The models with $\Delta\phi < M_{\text{pl}}$ are dubbed small-field inflation, in which case r is smaller than 2×10^{-3} for $N = 60$. In Ref. [20] the criterion $r = 10^{-2}$ was used to separate large-field and small-field models. Here we employ a more precise criterion according to Eq. (50).

Small-field inflation can be realized by the potential

$$V(\phi) = \Lambda^4 [1 - \mu(\phi)], \quad (51)$$

where Λ is a constant and $\mu(\phi)$ is a function of ϕ . In D-brane inflation [84] and Kähler-moduli inflation [85] we have $\mu(\phi) = e^{-\phi/M}$ and $\mu(\phi) = c_1\phi^{4/3}e^{-c_2\phi^{4/3}}$ ($c_1 > 0$, $c_2 > 0$), respectively. See Refs. [86] for other similar models.

For the function $f(\phi) = e^{-\phi/M}$ the number of e-foldings is given by $N \simeq (M/M_{\text{pl}})^2 e^{\phi/M}$, in which case n_s and r are

$$n_s \simeq 1 - \frac{2}{N}, \quad r \simeq \frac{8}{N^2} \left(\frac{M}{M_{\text{pl}}} \right)^2. \quad (52)$$

For $M < M_{\text{pl}}$ and $N = 60$, it follows that $n_s \simeq 0.967$ and $r < 2.2 \times 10^{-3}$. The model is inside the 68 % CL boundary constrained by the Planck+WP+BAO+high- ℓ data.

In Kähler-moduli inflation the inflationary observables are in the ranges $0.960 < n_s < 0.967$ and $r < 10^{-10}$ for $50 < N < 60$ [85], so the model belongs to a class of very small-field inflation. This model is consistent with the observational data as well.

4. Discrimination between general single-field models from observations

In this section we study observational constraints on single-field inflationary models that belong to the class of the Horndeski theory given by the action (1).

4.1. *k*-inflation

Kinetically driven inflation—called *k*-inflation [24]—corresponds to the action

$$S = \int d^4x \sqrt{-g} \left[\frac{M_{\text{pl}}^2}{2} R + P(\phi, X) \right], \quad (53)$$

i.e., $G_3 = G_4 = G_5 = 0$ in (1). Since $\epsilon = \epsilon_s = \delta_{P,X} = XP_{,X}/(M_{\text{pl}}^2 H^2)$, inflation occurs around either $X \approx 0$ or $P_{,X} \approx 0$. The former corresponds to slow-roll inflation discussed in Sec. 3, whereas the latter is *k*-inflation driven by the presence of non-linear terms in X .

From Eq. (16) the field propagation speed squared is given by [25]

$$c_s^2 = \frac{P_{,X}}{P_{,X} + 2XP_{,XX}}. \quad (54)$$

The observables (23) and (29) reduce to

$$n_s - 1 = -2\epsilon - \eta_s - s, \quad r = 16c_s\epsilon. \quad (55)$$

Since $\lambda/\Sigma = (1 - c_s^2)/2 + 2X^2 P_{,XXX} c_s^2 / (3P_{,X})$ [44], the equilateral leading-order non-linear parameter (34) reads

$$f_{\text{NL}}^{\text{equil}} = \frac{5}{324} \left(1 - \frac{1}{c_s^2} \right) (17 + 4c_s^2) - \frac{20}{243} \frac{X^2 P_{,XXX}}{P_{,X} + 2XP_{,XX}}. \quad (56)$$

If $c_s^2 \ll 1$, then $|f_{\text{NL}}^{\text{equil}}|$ can be much larger than 1.

To be concrete, we discuss the dilatonic ghost condensate model [87] characterized by the Lagrangian

$$P(\phi, X) = -X + e^{\alpha\phi/M_{\text{pl}}} X^2/M^4, \quad (57)$$

where α and M are constants. When $\alpha = 0$, this recovers the ghost condensate model [88]. Since $\epsilon = 3(2Xe^{\alpha\phi/M_{\text{pl}}} - M^4)/(3Xe^{\alpha\phi/M_{\text{pl}}} - M^4)$, $c_s^2 = (2Xe^{\alpha\phi/M_{\text{pl}}} - M^4)/(6Xe^{\alpha\phi/M_{\text{pl}}} - M^4)$, and $P_{,XXX} = 0$, the inflationary observables can be expressed as

$$n_s - 1 = n_t = -\frac{24c_s^2}{1 + 3c_s^2}, \quad r = \frac{192c_s^3}{1 + 3c_s^2}, \quad f_{\text{NL}}^{\text{equil}} = \frac{5}{324} \left(1 - \frac{1}{c_s^2} \right) (17 + 4c_s^2). \quad (58)$$

From the joint data analysis based on n_s and r , the sound speed is constrained as $0.034 < c_s < 0.046$ (95 % CL) from the Planck+WP+BAO+high- ℓ data [20]. Using an equilateral template of primordial non-Gaussianities, the Planck team derived the bound $c_s > 0.079$ (95 % CL). Hence the dilatonic ghost condensate model is disfavored by adding constraints from non-Gaussianities to those derived from n_s and r .

Let us consider the Dirac-Born-Infeld (DBI) model [89, 90] characterized by the Lagrangian

$$P(\phi, X) = -f(\phi)^{-1} \sqrt{1 - 2f(\phi)X} + f(\phi)^{-1} - V(\phi), \quad (59)$$

where $f(\phi)$ is a warp factor and $V(\phi)$ is a field potential. Since $\lambda/\Sigma = (1 - c_s^2)/(2c_s^2)$ in this case, the equilateral non-linear estimator (34) reads

$$f_{\text{NL}}^{\text{equil}} = \frac{35}{108} \left(1 - \frac{1}{c_s^2} \right). \quad (60)$$

Using this relation, the Planck team derived the bound $c_s > 0.07$ (95 % CL) [28]. The ultra-violet DBI models [89] correspond to the functions $f(\phi) \propto \phi^{-4}$ and $V(\phi) = m^2 \phi^2/2$. Taking

into account the bounds from n_s and r , this model is incompatible with the data for theoretically consistent model parameters [19, 91]. In the infrared DBI model characterized by $f(\phi) \propto \phi^{-4}$ and $V(\phi) = V_0 - \beta H^2 \phi^2/2$ [92] ($0.1 < \beta < 10^9$) the joint constraints from n_s , r , and $f_{\text{NL}}^{\text{equil}}$ restrict the allowed parameter space in a narrow range: $\beta < 0.7$ (95 % CL). In the power-law DBI model with the functions $f(\phi)^{-1} \propto e^{-\gamma\phi/M_{\text{pl}}}$ and $V(\phi) \propto e^{-\gamma\phi/M_{\text{pl}}}$ [93], the scalar propagation speed is contained as $0.07 < c_s < 0.43$ (95 % CL) from the bounds of n_s , r , and $f_{\text{NL}}^{\text{equil}}$ [20].

4.2. Starobinsky inflation

Let us consider the so-called $f(R)$ gravity described by the action

$$S = \int d^4x \sqrt{-g} \frac{M_{\text{pl}}^2}{2} f(R), \quad (61)$$

where $f(R)$ is an arbitrary function of R . This can be written as

$$S = \int d^4x \sqrt{-g} \left[\frac{1}{2} M_{\text{pl}} \phi R - V(\phi) \right], \quad \text{where} \quad \frac{\phi}{M_{\text{pl}}} = \frac{\partial f}{\partial R}, \quad V(\phi) = \frac{M_{\text{pl}}^2}{2} \left(R \frac{\partial f}{\partial R} - f \right). \quad (62)$$

Provided the function $f(R)$ includes non-linear terms of R , the scalar degree of freedom ϕ propagates. The field has a potential $V(\phi)$ of gravitational origin. We write (62) in a more general form

$$S = \int d^4x \sqrt{-g} \left[\frac{M_{\text{pl}}^2}{2} F(\phi) R + \omega(\phi) X - V(\phi) \right], \quad (63)$$

where $f(R)$ gravity corresponds to $F(\phi) = \phi/M_{\text{pl}}$ and $\omega(\phi) = 0$ [94]. Under the conformal transformation $\hat{g}_{\mu\nu} = F(\phi)g_{\mu\nu}$ we obtain the following action in the Einstein frame [95]:

$$\hat{S} = \int d^4x \sqrt{-\hat{g}} \left[\frac{1}{2} M_{\text{pl}}^2 \hat{R} - \frac{1}{2} \hat{g}^{\mu\nu} \partial_\mu \chi \partial_\nu \chi - U(\chi) \right], \quad (64)$$

where a hat represents quantities in the Einstein frame, and

$$U = \frac{V}{F^2}, \quad \chi = \int \mathcal{B}(\phi) d\phi, \quad \mathcal{B}(\phi) = \sqrt{\frac{3}{2} \left(\frac{M_{\text{pl}} F_{,\phi}}{F} \right)^2 + \frac{\omega}{F}}. \quad (65)$$

Let us consider the Starobinsky model [1]

$$f(R) = R + R^2/(6M^2). \quad (66)$$

In this case the field potential in the Einstein frame is given by

$$U(\chi) = \frac{3}{4} M^2 M_{\text{pl}}^2 \left(1 - e^{-\sqrt{2/3} \chi/M_{\text{pl}}} \right)^2, \quad \text{where} \quad \chi = \sqrt{\frac{3}{2}} M_{\text{pl}} \ln \left(1 + \frac{R}{3M^2} \right). \quad (67)$$

In the limit that $\chi \rightarrow \infty$ the potential approaches a constant $U(\chi) \rightarrow 3M^2 M_{\text{pl}}^2/4$, so that inflation occurs in the regime $\chi \gg M_{\text{pl}}$. The slow-roll parameters $\hat{\epsilon}_V$ and $\hat{\eta}_V$ in this regime can be estimated as $\hat{\epsilon}_V \simeq 3/(4N^2)$ and $\hat{\eta}_V \simeq -1/N$, where $N \simeq (3/4)e^{\sqrt{2/3}\chi/M_{\text{pl}}}$ is the number of e-foldings. In Refs. [96] it was shown that the inflationary power spectra of scalar and

tensor perturbations in the original (Jordan) frame are equivalent to those in the Einstein frame. From Eq. (39) the inflationary observables are [97]

$$n_s = 1 - \frac{2}{N}, \quad r = \frac{12}{N^2}. \quad (68)$$

When $N = 60$ we have $n_s = 0.967$ and $r = 0.0033$. As we see in Fig. 1, the Starobinsky model is well inside the 68 % CL contour constrained by the Planck+WP+BAO+high- ℓ data. See Refs. [98] for theoretical attempts to construct the Starobinsky model in the framework of supergravity and quantum gravity.

4.3. Higgs inflation

From the amplitude of the CMB anisotropies the typical mass scale of inflation is around $H \sim 10^{14}$ GeV [19]. This is much higher than the electroweak scale ($\sim 10^2$ GeV), so the Higgs field cannot be responsible for inflation in its simplest form. However, this situation is subject to change in the presence of non-minimal couplings or other interactions. In what follows we briefly review a number of approaches to accommodate the Higgs field for inflation and discriminate those models from observations.

4.3.1. Non-minimal couplings. The models with non-minimal couplings between the inflaton and the Ricci scalar are described by the action [29, 30]

$$S = \int d^4x \sqrt{-g} \left[\frac{M_{\text{pl}}^2}{2} R - \frac{1}{2} \xi \phi^2 R + X - V(\phi) \right], \quad (69)$$

where the conformal coupling corresponds to $\xi = 1/6$. The model (69) corresponds to $F(\phi) = 1 - \xi \phi^2/M_{\text{pl}}^2$ and $\omega(\phi) = 1$ in (63). Then the action in the Einstein frame is given by (64) with the potential $U = V/F^2$. The Higgs potential $V(\phi) = (\lambda_4/4)(\phi^2 - v^2)^2$ ($v \sim 10^2$ GeV) can be approximated as $V(\phi) \simeq \lambda_4 \phi^4/4$ during inflation ($\phi^2 \gg v^2$). Then the potential in the Einstein frame reads

$$U \simeq \frac{\lambda_4 \phi^4}{4(1 - \xi \phi^2/M_{\text{pl}}^2)^2}. \quad (70)$$

For negative ξ , the potential is asymptotically flat in the regime $-\xi \phi^2/M_{\text{pl}}^2 \gg 1$.

Let us consider the case of a large negative non-minimal coupling ($|\xi| \gg 1$). The scalar power spectrum (22) can be estimated as $\mathcal{P}_\zeta \simeq \lambda_4 N^2/(72\pi^2 \xi^2)$ with $N \simeq -(3/4)\xi \phi^2/M_{\text{pl}}^2$. Using the Planck normalization $\mathcal{P}_\zeta = 2.2 \times 10^{-9}$ [19, 20] with $N = 60$, we obtain $\lambda_4/\xi^2 \simeq -4.3 \times 10^{-10}$. For the non-minimal coupling $\xi \approx -10^4$, the self coupling λ_4 can be of the order of 0.1. Since the slow-roll parameters in the Einstein frame are given by $\epsilon_V \simeq (4/3)(M_{\text{pl}}^2/(\xi \phi^2))^2$ and $\eta_V \simeq 4M_{\text{pl}}^2/(3\xi \phi^2)$ [99], we obtain

$$n_s \simeq 1 - \frac{2}{N}, \quad r \simeq \frac{12}{N^2} \quad (|\xi| \gg 1). \quad (71)$$

Provided that quantum corrections to the tree-level action are suppressed, the theoretical values (71) are the same as those in the Starobinsky model, so the model is within the 68 % CL observational contour.

A detailed analysis shows that the non-minimal coupling is constrained as $\xi < -4.5 \times 10^{-3}$ (68 % CL) from the joint data analysis of Planck+WP+BAO+high- ℓ [20].

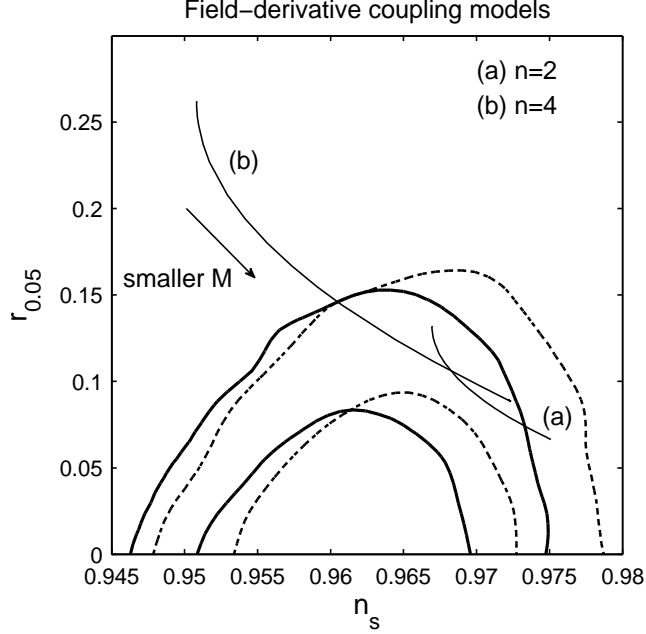


Fig. 2 Observational constraints on field-derivative coupling models (72) for the monomial potential $V(\phi) = \lambda_n \phi^n/n$. The thick solid and dotted curves show the 68 % CL (inside) and 95 % CL (outside) boundaries derived by the joint data analyses of Planck+WP+BAO+high- ℓ and Planck+WP+BAO, respectively. The thin solid curves correspond to the theoretical predictions of the models $n = 2$ and $n = 4$, respectively (for $N = 60$). For decreasing M the scalar spectral index gets larger, whereas the tensor-to-scalar ratio becomes smaller.

4.3.2. *Field-derivative couplings to the Einstein tensor.* Let us proceed to the field-derivative coupling model described by the action [37]

$$S = \int d^4x \sqrt{-g} \left[\frac{M_{\text{pl}}^2}{2} R + X - V(\phi) + \frac{1}{2M^2} G^{\mu\nu} \partial_\mu \phi \partial_\nu \phi \right], \quad (72)$$

where M is a constant having a dimension of mass. In the regime where the Hubble parameter H is larger than M , the field evolves more slowly relative to the case of standard inflation due to a gravitationally enhanced friction².

For a slow-rolling field satisfying the condition $\varepsilon = \dot{\phi}^2/(M^2 M_{\text{pl}}^2) \ll 1$, the strong coupling scale Λ_c of the derivative coupling theory is as close as the Planck scale M_{pl} [37]. This comes from the fact that an asymptotic local shift symmetry (related to the Galilean symmetry mentioned later in Sec. 4.3.3) is only softly broken for $\varepsilon \ll 1$, so that the potential can be protected against quantum corrections during inflation even in the regime $M < H < M_{\text{pl}}$ [100]. Note that the sign of the last term of Eq. (72) has been chosen to avoid the appearance of ghosts.

²This property is similar to what happens for warm inflation [101], in which dissipative processes lead to an effective friction for the inflaton.

To be concrete, let us consider the monomial potential given in (42). In this case, Eqs. (23) and (29) read [102, 103]

$$n_s = 1 - \frac{n^2[n(n+2) + 2(n+1)\alpha y^n]}{y^2(n + \alpha y^n)^2}, \quad r = \frac{8n^3}{y^2(n + \alpha y^n)}, \quad (73)$$

where $\alpha = \lambda_n M_{\text{pl}}^{n-2}/M^2$ and $y = \phi/M_{\text{pl}}$. The number of e-foldings is given by $N = y^2[1 + 2\alpha y^n/(n(n+2))]/(2n) - y_f^2[1 + 2\alpha y_f^n/(n(n+2))]/(2n)$, where y_f is known by solving $2y_f^2(1 + \alpha y_f^n/n) = n^2$. In the limit $\alpha \rightarrow \infty$, it follows that

$$n_s = 1 - \frac{4(n+1)}{2(n+2)N + n}, \quad r = \frac{16n}{2(n+2)N + n}. \quad (74)$$

If $N = 60$, then $n_s = 0.975$, $r = 0.066$ for $n = 2$ and $n_s = 0.972$, $r = 0.088$ for $n = 4$.

In Fig. 2 we plot theoretical curves in the (n_s, r) plane for $n = 2$ and $n = 4$ in the parameter range $10^{-8} \leq \alpha \leq 10^8$. Although r gets smaller for decreasing M due to the enhanced gravitational friction, both potentials are outside the 68% CL region. In the limit $\alpha \rightarrow \infty$, the potential $V(\phi) = \lambda_4 \phi^4/4$ is marginally inside the 95% CL contour. From the joint data analysis of Planck+WP+BAO+high- ℓ , the same potential is inside the 95% CL boundary for $\alpha > 9.0 \times 10^{-5}$ [20].

In the regime $H \gg M$ the scalar power spectrum is approximately given by $\mathcal{P}_\zeta \simeq V^4/(12\pi^2 M_{\text{pl}}^8 M^2 V_{,\phi}^2)$. Using the Planck normalization $\mathcal{P}_\zeta \simeq 2.2 \times 10^{-9}$ at $N = 60$, the self coupling is constrained as $\lambda_4 \simeq 6 \times 10^{-32} (M_{\text{pl}}/M)^4$. For $M \simeq 3 \times 10^{-8} M_{\text{pl}}$ it is possible to realize $\lambda_4 \simeq 0.1$.

4.3.3. Galileon self-interactions. The field equations of motion following from the Lagrangian $X \square \phi$ are invariant under the Galilean shift $\partial_\mu \phi \rightarrow \partial_\mu \phi + b_\mu$ in the limit of Minkowski space-time [32]. The general covariant Galileons [33] having the same property as the term $X \square \phi$ can be accommodated by the action (1) with the choice

$$P = X - V(\phi), \quad G_3 = \frac{c_3}{M^3} X, \quad G_4 = -\frac{c_4}{M^6} X^2, \quad G_5 = \frac{3c_5}{M^9} X^2, \quad (75)$$

where only the linear potential $V(\phi) \propto \phi$ is allowed to respect the Galilean symmetry in the limit of Minkowski space-time. In the following we do not restrict the form of the field potential to the linear one since the Galilean symmetry is broken in the curved space-time anyway. In the presence of the terms G_3, G_4, G_5 given in Eq. (75) the evolution of the inflaton along the potential also slows down [104]. For simplicity, let us consider the case where the terms G_4 and G_5 are absent. From Eqs. (14) and (16) we have

$$q_s = \delta_{PX} + 6\delta_{G_3X}, \quad c_s^2 = \frac{\delta_{PX} + 4\delta_{G_3X}}{\delta_{PX} + 6\delta_{G_3X}}, \quad (76)$$

where $\delta_{G_3X} = c_3 \dot{\phi} X / (M^3 M_{\text{pl}}^2 H)$. When $|\delta_{G_3X}| \gg \delta_{PX}$ the Galileon self-interaction dominates over the standard kinetic term. In this regime, the avoidance of ghosts requires the condition $\delta_{G_3X} > 0$, i.e., $c_3 \dot{\phi} > 0$. The propagation speed squared is approximately given by $c_s^2 \simeq 2/3$, so that the Laplacian instability can be avoided during inflation. Since $r = 16(\delta_{PX} + 4\delta_{G_3X})^{3/2}/(\delta_{PX} + 6\delta_{G_3X})^{1/2}$ and $n_t = -2(\delta_{PX} + 3\delta_{G_3X})$, the consistency relation in the regime $|\delta_{G_3X}| \gg \delta_{PX}$ is given by $r \simeq -8.7n_t$.

Let us consider the monomial potential (42). In the regime where M is much smaller than H , the observables (23) and (29) reduce to [104, 105]

$$n_s = 1 - \frac{3(n+1)}{(n+3)N+n}, \quad r = \frac{64\sqrt{6}}{9} \frac{n}{(n+3)N+n}, \quad (77)$$

which give $n_s = 0.965$ and $r = 0.164$ for $n = 4$ and $N = 60$. For intermediate values of M the tensor-to-scalar ratio of the potential $V(\phi) = \lambda_4 \phi^4/4$ is in the range $0.164 < r < 0.262$ for $N = 60$, in which case the model is outside the 95 % CL boundary constrained by the Planck+WP+BAO+high- ℓ data [20]. For the Galileon couplings $G_4 = -c_4 X^2/M^6$ or $G_5 = 3c_5 X^2/M^9$ the self-coupling potential enters the 95 % CL contour in the presence of Galileon terms, but it is still outside the 68 % CL contour [20]. The quadratic potential $V(\phi) = m^2 \phi^2/2$ is also outside the 68 % CL boundary.

If the Galileon term dominates over the standard kinetic term even after inflation, this gives rise to instabilities associated with the appearance of negative c_s^2 during reheating [105]. This provides a lower bound on the mass scale M of $M \gtrsim 10^{-4} M_{\text{pl}} \approx 10^{14}$ GeV for the monomial potential (42). This lower bound is similar to the typical energy scale of inflation. Hence the Hubble parameter H is not actually much larger than M during inflation. Even for $H \sim M$, however, n_s and r are close to the values (77) [105].

5. Anisotropic inflation

The WMAP data showed that there may be some anomalies related to the broken rotational invariance of the CMB perturbations [48]. The power spectrum of curvature perturbations with broken statistical isotropy can be parametrized as

$$\mathcal{P}_\zeta(\mathbf{k}) = \mathcal{P}_\zeta^{(0)}(k) (1 + g_* \cos^2 \theta_{\mathbf{k}, \mathbf{V}}), \quad (78)$$

where $\mathcal{P}_\zeta^{(0)}(k)$ is the isotropic power spectrum, g_* quantifies the deviation from the isotropy, \mathbf{V} is a privileged direction close to the ecliptic poles, and $\theta_{\mathbf{k}, \mathbf{V}}$ is the angle between the wavenumbers \mathbf{k} and \mathbf{V} . From the WMAP5 data, Groeneboom *et al.* [49] derived the bound $g_* = 0.29 \pm 0.031$ with the exclusion of $g_* = 0$ at 9σ . From the Planck data the bound $g_* = 0.002 \pm 0.016$ (68% CL) was recently derived by Kim and Komatsu [51] after eliminating the asymmetry of the beam and the Galactic foreground emission. Although the isotropic spectrum is consistent with the Planck data, the anisotropy of the order $|g_*| = 0.01$ has not yet been excluded.

In order to explain the origin of statistical anisotropies, we need to go beyond the simplest single-field inflationary scenario. If the inflaton couples to a vector field with a kinetic term $F_{\mu\nu} F^{\mu\nu}$, the anisotropic hair can survive during inflation for a suitable choice of coupling $f^2(\phi)$ [52]. In the following we review the mechanism of anisotropic inflation and evaluate the anisotropy parameter g_* as well as the non-linear parameter f_{NL} in such a scenario.

5.1. Anisotropic hair

We start with the following action

$$S = \int d^4x \sqrt{-g} \left[\frac{M_{\text{pl}}^2}{2} R + X - V(\phi) - \frac{1}{4} f^2(\phi) F_{\mu\nu} F^{\mu\nu} \right], \quad (79)$$

where the field strength of the vector field is characterized by $F_{\mu\nu} = \partial_\mu A_\nu - \partial_\nu A_\mu$. Choosing the gauge $A_0 = 0$, the x -axis can be taken for the direction of the vector, i.e., $A_\mu =$

$(0, v(t), 0, 0)$, where $v(t)$ is a function with respect to t . There is rotational symmetry in the (y, z) plane, so that the line element can be expressed as

$$ds^2 = -\mathcal{N}^2(t)dt^2 + e^{2\alpha(t)} \left[e^{-4\sigma(t)} dx^2 + e^{2\sigma(t)} (dy^2 + dz^2) \right], \quad (80)$$

where $\mathcal{N}(t)$ is the lapse function, and $e^\alpha \equiv a$ and σ are the isotropic scale factor and the spatial shear, respectively. Then the action (79) can be written as

$$S = \int d^4x \frac{e^{3\alpha}}{\mathcal{N}} \left[3M_{\text{pl}}^2 (\dot{\sigma}^2 - \dot{\alpha}^2) + \frac{1}{2} \dot{\phi}^2 - \mathcal{N}^2 V(\phi) + \frac{1}{2} f^2(\phi) e^{-2\alpha+4\sigma} \dot{v}^2 \right]. \quad (81)$$

The equation of motion for v following from the action (81) can be integrated to give

$$\dot{v} = p_A f^{-2}(\phi) e^{-\alpha-4\sigma}, \quad (82)$$

where p_A is a constant. Varying the action (81) with respect to \mathcal{N} , α , σ , ϕ , and setting $\mathcal{N} = 1$, we obtain

$$H^2 = \dot{\sigma}^2 + \frac{1}{3M_{\text{pl}}^2} \left[\frac{1}{2} \dot{\phi}^2 + V(\phi) + \rho_A \right], \quad (83)$$

$$\dot{H} = -3\dot{\sigma}^2 - \frac{1}{M_{\text{pl}}^2} \left(\frac{1}{2} \dot{\phi}^2 + \frac{2}{3} \rho_A \right), \quad (84)$$

$$\ddot{\sigma} = -3H\dot{\sigma} + \frac{2\rho_A}{3M_{\text{pl}}^2}, \quad (85)$$

$$\ddot{\phi} + 3H\dot{\phi} + V_{,\phi}(\phi) - p_A^2 f^{-3}(\phi) f_{,\phi}(\phi) e^{-4\alpha-4\sigma} = 0, \quad (86)$$

where $H = \dot{\alpha}$, and the energy density of the vector field is given by

$$\rho_A \equiv \frac{1}{2} p_A^2 f^{-2}(\phi) e^{-4\alpha-4\sigma}. \quad (87)$$

The inflaton energy density $\rho_\phi \equiv \dot{\phi}^2/2 + V(\phi)$ needs to be much larger than ρ_A to sustain inflation. Moreover, the Hubble parameter H should be much larger than the shear term $\Sigma \equiv \dot{\sigma}$, so that Eq. (83) is approximately given by $H^2 \simeq \rho_\phi/(3M_{\text{pl}}^2)$. From Eq. (84) the slow-roll parameter $\epsilon = -\dot{H}/H^2$ is much smaller than 1 under the condition $\dot{\phi}^2/2 \ll V(\phi)$. If the shear Σ approaches a constant value, Eq. (85) shows that the ratio Σ/H converges to

$$\frac{\Sigma}{H} \simeq \frac{2\rho_A}{3V}. \quad (88)$$

In order to keep the energy density ρ_A nearly constant, we require that

$$f(\phi) \simeq e^{-2\alpha} = a^{-2}, \quad (89)$$

where we used the property $|\sigma| \ll \alpha$. Neglecting the contribution of the vector field and the $\ddot{\phi}$ term on the l.h.s. of Eq. (86), we obtain $3\dot{\alpha}\dot{\phi} \simeq -V_{,\phi}$ and hence $d\alpha/d\phi \simeq -V/(M_{\text{pl}}^2 V_{,\phi})$.

Integrating this equation, the critical coupling (89) can be expressed as

$$f(\phi) = e^{2 \int \frac{V}{M_{\text{pl}}^2 V, \phi} d\phi}. \quad (90)$$

Let us substitute Eq. (90) for Eq. (86) and drop the $\ddot{\phi}$ term alone, i.e.,

$$\frac{d\phi}{d\alpha} \simeq -\frac{M_{\text{pl}}^2 V, \phi}{V} + \frac{2p_A^2}{V, \phi} e^{-4\alpha - 4\sigma - 4 \int \frac{V}{M_{\text{pl}}^2 V, \phi} d\phi}. \quad (91)$$

Neglecting the variation of ϕ/M_{pl} relative to that of α , this equation can be integrated to give

$$e^{4\alpha + 4\sigma + 4 \int \frac{V}{M_{\text{pl}}^2 V, \phi} d\phi} \simeq \frac{8p_A^2 V}{M_{\text{pl}}^2 V, \phi^2} (\alpha + \alpha_0), \quad (92)$$

where $\alpha_0 > 0$ is an integration constant. Substituting Eqs. (90) and (92) into Eq. (87), we obtain the following relation

$$r_A \equiv \frac{\rho_A}{\epsilon V} \simeq \frac{1}{8(\alpha + \alpha_0)}, \quad (93)$$

where we have used the property $\epsilon \simeq (M_{\text{pl}}^2/2)(V, \phi/V)^2$ under the slow-roll approximation. As long as $\alpha \ll \alpha_0$, the ratio r_A stays nearly constant. From Eq. (88) and (93) we have

$$\frac{\Sigma}{H} \simeq \frac{\epsilon}{12(\alpha + \alpha_0)}, \quad (94)$$

so that the anisotropic hair survives for $\alpha \ll \alpha_0$.

We can generalize the above discussion to the more general coupling $f(\phi) = e^{2c \int \frac{V}{M_{\text{pl}}^2 V, \phi} d\phi}$, where c is a constant. When $c > 1$, there is an attractor solution along which the anisotropic hair survives during inflation. Along this attractor the shear to the Hubble parameter is given by $\Sigma/H \simeq (c-1)\epsilon/(3c)$ [52].

5.2. Anisotropic power spectra

For the anisotropic inflationary scenario described by the action (79), let us derive the scalar power spectrum in the form (78). Since the anisotropy of the expansion rate should be sufficiently small for compatibility with observations, we can ignore the effect of the anisotropic expansion for the derivation of the perturbation equations [55]. Then we use the perturbed metric (10) with the curvature perturbation ζ defined in Eq. (11). We choose the spatially flat gauge ($\psi = 0$), so that $\zeta = -(H/\dot{\phi})\delta\phi$.

The curvature perturbation is decomposed into the isotropic field $\zeta^{(0)}$ and the anisotropic contribution $\delta\zeta$, as $\zeta = \zeta^{(0)} + \delta\zeta$. Decomposing ζ into the Fourier components as Eq. (17), the solution to the isotropic component $\zeta^{(0)}(\tau, k)$ is given by Eq. (20) with $c_s^2 = 1$ and $Q_s = M_{\text{pl}}^2 \epsilon$. From Eq. (22) the isotropic scalar power spectrum is

$$\mathcal{P}_\zeta^{(0)} = \frac{H^2}{8\pi^2 M_{\text{pl}}^2 \epsilon}, \quad (95)$$

which is evaluated at $k = aH$.

In the Coulomb gauge, the vector field A_μ can be decomposed into the Fourier components,

$$A_i(\mathbf{x}, \tau) = A_i^{(0)}(\tau) + \delta A_i, \\ \delta A_i = \sum_{\lambda=1,2} \int \frac{d^3k}{(2\pi)^{3/2}} e^{i\mathbf{k}\cdot\mathbf{x}} \left[A_\lambda(k, \tau) a_\lambda(\mathbf{k}) + A_\lambda^*(k, \tau) a_\lambda^\dagger(-\mathbf{k}) \right] \epsilon_i^{(\lambda)}(\mathbf{k}), \quad (96)$$

where $A_i^{(0)}(\tau) = (A_x^{(0)}, 0, 0)$ is the background component, and $\epsilon_i^{(\lambda)}(\mathbf{k})$ ($\lambda = 1, 2$) are polarization vectors satisfying the relations $k_i \epsilon_i^{(\lambda)}(\mathbf{k}) = 0$, $\epsilon_i^{(\lambda)}(-\mathbf{k}) = \epsilon_i^{*(\lambda)}(\mathbf{k})$, and $\epsilon_i^{(\lambda)}(\mathbf{k}) \epsilon_i^{*(\lambda')}(\mathbf{k}) = \delta_{\lambda\lambda'}$. Introducing a rescaled field $V_\lambda = f A_\lambda$, it obeys the equation of motion

$$V_\lambda'' + \left(k^2 - \frac{f''}{f} \right) V_\lambda = 0. \quad (97)$$

In the following, let us focus on the coupling (89). Since $f \propto \tau^2$ on the de Sitter background ($a = -(\tau H)^{-1}$), it follows that $f''/f = 2/\tau^2$. In this case, the vector-field perturbation is scale-invariant. Imposing the Bunch-Davies vacuum in the asymptotic past, the solution to Eq. (97) is given by

$$A_\lambda(k, \tau) = \frac{H a^3}{\sqrt{2k^3}} (1 + ik\tau) e^{-ik\tau}. \quad (98)$$

On the flat FLRW background with the line element $ds^2 = a^2(-d\tau^2 + \delta_{ij} dx^i dx^j)$, the tree-level interacting Lagrangian $L_{\text{int}} = -\sqrt{-g} f^2(\phi) F_{\mu\nu} F^{\mu\nu} / 4$ can be expanded up to second order in perturbations with the expansion $f^2 = \bar{f}^2 + (\partial \bar{f}^2 / \partial \phi) \delta\phi$ and $F_{\mu\nu} = \bar{F}_{\mu\nu} + \delta F_{\mu\nu}$ (a bar represents background values). On using the property $(\partial \bar{f}^2 / \partial \phi) \delta\phi = 4f^2 \zeta$ in the spatially flat gauge, the second-order interacting Lagrangian for curvature perturbations reads

$$L_{\text{int}}^{(2)} = 4a^4 E_x \delta E_x \zeta, \quad (99)$$

where $E_x = f A_x^{(0)'} / a^2$ and $\delta E_i = f \delta A_i' / a^2$. From (98) the solution to $\delta E_i(\mathbf{x}, \tau)$ in the super-Hubble regime ($|k\tau| \ll 1$) can be expressed as

$$\delta E_i(\mathbf{x}, \tau) = \int \frac{d^3k}{(2\pi)^{3/2}} e^{i\mathbf{k}\cdot\mathbf{x}} \delta \hat{E}_i(\mathbf{k}, \tau), \quad \delta \hat{E}_i(\mathbf{k}, \tau) = \sum_{\lambda=1,2} \frac{3H^2}{\sqrt{2k^3}} \left[a_\lambda(\mathbf{k}) + a_\lambda^\dagger(-\mathbf{k}) \right] \epsilon_i^{(\lambda)}(\mathbf{k}). \quad (100)$$

Then, the interacting Hamiltonian $H_\zeta = -\int d^3x L_{\text{int}}^{(2)}$ is given by

$$H_\zeta = -\frac{4E_x}{H^4 \tau^4} \int d^3k \delta \hat{E}_x(\mathbf{k}, \tau) \hat{\zeta}^{(0)}(-\mathbf{k}, \tau). \quad (101)$$

From this we can compute the contribution to the two-point correlation function of scalar perturbations, as

$$\begin{aligned} \delta \langle 0 | \hat{\zeta}(\mathbf{k}_1) \hat{\zeta}(\mathbf{k}_2) | 0 \rangle &= - \int_{\tau_{\text{min},1}}^{\tau} d\tau_1 \int_{\tau_{\text{min},2}}^{\tau_1} d\tau_2 \langle 0 | \left[\left[\hat{\zeta}^{(0)}(\mathbf{k}_1, \tau) \hat{\zeta}^{(0)}(\mathbf{k}_2, \tau), H_\zeta(\tau_1) \right], H_\zeta(\tau_2) \right] | 0 \rangle \\ &= \frac{4E_x^2}{9\epsilon^2 M_{\text{pl}}^4 H^4} \prod_{i=1}^2 \int_{-1/k_i}^{\tau} \frac{d\tau_i}{\tau_i^4} (\tau^3 - \tau_i^3) \langle 0 | \delta \hat{E}_x(\mathbf{k}_1, \tau_1) \delta \hat{E}_x(\mathbf{k}_2, \tau_2) | 0 \rangle \\ &= \frac{2\pi^2}{k_1^3} \delta^{(3)}(\mathbf{k}_1 + \mathbf{k}_2) \frac{E_x^2 N_k^2 \sin^2 \theta_{\mathbf{k}_1, \mathbf{x}}}{\pi^2 \epsilon^2 M_{\text{pl}}^4}, \end{aligned} \quad (102)$$

where we have used the property

$$[\hat{\zeta}^{(0)}(\mathbf{k}, \tau), \hat{\zeta}^{(0)}(\mathbf{k}', \tau')] \simeq -i \frac{H^2}{6\epsilon M_{\text{pl}}^2} (\tau^3 - \tau'^3) \delta^{(3)}(\mathbf{k} + \mathbf{k}'). \quad (103)$$

In the first line of Eq. (102) we have evaluated the two integrals in the super-horizon regime ($-k_i\tau < 1$), i.e., $\tau_{\min,i} = -1/k_i$ with $i = 1, 2$. We also employed the relation $\int_{-1/k_i}^{\tau} d\tau_i (\tau^3 - \tau_i^3)/\tau_i^4 \simeq \ln(aH/k_i) \simeq N_{k_i}$ in the regime $-k_i\tau \ll 1$, where N_{k_i} is the number of e-foldings before the end of inflation at which the modes with the wavenumber k_i left the Hubble radius. Since $\mathbf{k}_1 = -\mathbf{k}_2$, it follows that $N_{k_1} = N_{k_2} \equiv N_k$.

From Eqs. (95) and (102), the total scalar power spectrum is given by

$$\mathcal{P}_\zeta = \mathcal{P}_\zeta^{(0)} (1 + 48r_A N_k^2 \sin^2 \theta_{\mathbf{k}_1, \mathbf{x}}) , \quad (104)$$

where we have used the relation $\rho_A = E_x^2/2$ and the definition r_A given in Eq. (93). Comparing the spectrum (104) with the parametrization (78), it follows that

$$g_* = -48 r_A N_k^2 = -48 \frac{\rho_A}{\epsilon V} N_k^2 . \quad (105)$$

Since $g_* < 0$, the power spectrum has an oblate-type anisotropy. The condition $|g_*| \lesssim 0.01$ translates to $r_A \lesssim 10^{-7}$ for $N_k \sim 60$. In Eq. (93) the parameter α corresponds to the number of e-foldings from the onset of inflation, so that $r_A \simeq 1/(8\alpha_0) = \text{constant}$ for $\alpha \ll 10^6$. Thus, the model (79) with the coupling (89) can explain the broken rotational invariance of the scalar power spectrum.

The tensor power spectrum can be computed in a similar way from the interacting Hamiltonian with the vector field A_i and the tensor perturbation h_{ij} . It is given by [55, 59]

$$\mathcal{P}_h = 16\epsilon \mathcal{P}_\zeta^{(0)} (1 + 12\epsilon r_A N_k^2 \sin^2 \theta_{\mathbf{k}_1, \mathbf{x}}) . \quad (106)$$

Compared to the scalar spectrum (104), the anisotropic contribution is suppressed due to the additional factor ϵ . Then the presence of anisotropies leads to the suppressed tensor-to-scalar ratio $r = \mathcal{P}_h/\mathcal{P}_\zeta$. For increasing N_k , the scalar amplitude \mathcal{P}_ζ gets larger, which leads to the decrease of n_s . If $|g_*|$ is larger than the order of 0.1, observational constraints on inflaton potentials in the (n_s, r) plane are subject to change [59].

5.3. Primordial non-Gaussianities

We also compute the three-point correlation function of curvature perturbations for the coupling (89). In addition to the second-order interacting Lagrangian $L_{\text{int}}^{(2)}$, there is a contribution to the bispectrum coming from the third-order interacting Lagrangian $L_{\text{int}}^{(3)} \simeq 2a^4 \delta E_i \delta E_j \zeta$. The corresponding interacting Hamiltonian is given by

$$H_{\zeta^2} = -\frac{2}{H^4 \tau^4} \int \frac{d^3 k d^3 p}{(2\pi)^{3/2}} \delta \hat{E}_i(\mathbf{k}, \tau) \delta \hat{E}_j(\mathbf{p}, \tau) \hat{\zeta}^{(0)}(-\mathbf{k} - \mathbf{p}, \tau) . \quad (107)$$

Then the three-point correlation of ζ can be evaluated as [57]

$$\begin{aligned} \delta \langle 0 | \hat{\zeta}(\mathbf{k}_1) \hat{\zeta}(\mathbf{k}_2) \hat{\zeta}(\mathbf{k}_3) | 0 \rangle &= i \int_{\tau_{\min,1}}^{\tau} d\tau_1 \int_{\tau_{\min,2}}^{\tau_1} d\tau_2 \int_{\tau_{\min,3}}^{\tau_2} d\tau_3 \\ &\times \langle 0 | \left[\left[\left[\hat{\zeta}^{(0)}(\mathbf{k}_1) \hat{\zeta}^{(0)}(\mathbf{k}_2) \hat{\zeta}^{(0)}(\mathbf{k}_3)(\tau), H_{\zeta^2}(\tau_1) \right], H_{\zeta}(\tau_2) \right] H_{\zeta}(\tau_3) \right] | 0 \rangle + 2 \text{ permutations} \\ &\simeq 288 \sqrt{2} \pi^{5/2} \frac{E_x^2}{\epsilon V} N_{k_1} N_{k_2} N_{k_3} (\mathcal{P}_\zeta^{(0)})^2 \delta^{(3)}(\mathbf{k}_1 + \mathbf{k}_2 + \mathbf{k}_3) \\ &\times \left[\frac{1}{k_1^3 k_2^3} (1 - \cos^2 \theta_{\mathbf{k}_1, \mathbf{x}} - \cos^2 \theta_{\mathbf{k}_2, \mathbf{x}} + \cos \theta_{\mathbf{k}_1, \mathbf{x}} \cos \theta_{\mathbf{k}_2, \mathbf{x}} \cos \theta_{\mathbf{k}_1, \mathbf{k}_2}) + 2 \text{ permutations} \right] . \end{aligned} \quad (108)$$

The nonlinear parameter f_{NL} following from the bispectrum (108) reads [57]

$$f_{\text{NL}} = 6 \left(\frac{-g_*}{0.01} \right) \left(\frac{N_k}{60} \right) \frac{1}{k_1^3 + k_2^3 + k_3^3} [k_3^3 (1 - \cos^2 \theta_{\mathbf{k}_1, \mathbf{x}} - \cos^2 \theta_{\mathbf{k}_2, \mathbf{x}} + \cos \theta_{\mathbf{k}_1, \mathbf{x}} \cos \theta_{\mathbf{k}_2, \mathbf{x}} \cos \theta_{\mathbf{k}_1, \mathbf{k}_2}) + 2 \text{ permutations}], \quad (109)$$

where we have used the approximations $(\mathcal{P}_\zeta)^2 \simeq (\mathcal{P}_\zeta^{(0)})^2$ and $N_{k_1} \simeq N_{k_2} \simeq N_{k_3} \equiv N_k$.

In the strict squeezed limit characterized by $k_3 \rightarrow 0$ and $\theta_{\mathbf{k}_1, \mathbf{k}_2} \rightarrow \pi$, the nonlinear estimator f_{NL} vanishes for any values of $\theta_{\mathbf{k}_1, \mathbf{x}}$ [59]. This corresponds to the case in which the angles $\theta_{\mathbf{k}_2, \mathbf{k}_3}$ and $\theta_{\mathbf{k}_3, \mathbf{k}_1}$ approach $\pi/2$. For the incomplete squeezed shape where the angles $\theta_{\mathbf{k}_2, \mathbf{k}_3}$ and $\theta_{\mathbf{k}_3, \mathbf{k}_1}$ are not necessarily close to $\pi/2$, we can take any angle between \mathbf{k}_3 and $\mathbf{k}_1, \mathbf{k}_2$. Averaging over f_{NL} in all the directions, the nonlinear estimator of the squeezed shape ($k_3 \ll k_1 \simeq k_2$, $\theta_{\mathbf{k}_1, \mathbf{k}_3} \rightarrow \pi - \theta_{\mathbf{k}_2, \mathbf{k}_3}$, and $\theta_{\mathbf{k}_2, \mathbf{x}} \rightarrow \pi - \theta_{\mathbf{k}_1, \mathbf{x}}$) can be estimated as [57]

$$f_{\text{NL}}^{\text{local, average}} \simeq 2.7 \left(\frac{-g_*}{0.01} \right) \left(\frac{N_k}{60} \right) \frac{[1 - \cos^2 \theta_{\mathbf{k}_1, \mathbf{x}} - \cos^2 \theta_{\mathbf{k}_3, \mathbf{x}} + \cos \theta_{\mathbf{k}_1, \mathbf{x}} \cos \theta_{\mathbf{k}_3, \mathbf{x}} \cos \theta_{\mathbf{k}_1, \mathbf{k}_3}]}{4/9}, \quad (110)$$

where we have used the fact that the average of the function in the last square bracket integrated over all the angles is $4/9$. If $g_* = -0.01$ and $N = 60$, then $f_{\text{NL}}^{\text{local, average}} = 2.7$ and hence the model can be compatible with the Planck bound $f_{\text{NL}}^{\text{local}} = 2.7 \pm 5.8$ (68 % CL). In the equilateral limit ($k_1 = k_2 = k_3$) the non-linear estimator (109) reduces to

$$f_{\text{NL}}^{\text{equil}} \simeq 0.75 \left(\frac{-g_*}{0.01} \right) \left(\frac{N_k}{60} \right), \quad (111)$$

which is smaller than the order of 1 for $|g_*| < 0.01$.

5.4. Generality of anisotropic inflation

So far we have focused on the case of potential-driven anisotropic slow-roll inflation, but the anisotropic hair can also survive in other inflationary scenarios. For example, in k-inflation, the power-law cosmic acceleration ($a \propto t^p$ with $p > 1$) can be realized for the Lagrangian $P = Xg(Y)$ [87, 106], where g is an arbitrary function in terms of $Y = Xe^{\lambda\phi/M_{\text{Pl}}}$ (λ is a constant). If the inflaton couples to the vector field A_μ with an exponential coupling $f(\phi) \propto e^{\mu\phi/M_{\text{Pl}}}$, the models with the Lagrangian $P = Xg(Y)$ give rise to anisotropic inflationary solutions with $\Sigma/H = \text{constant}$ [107]. Moreover, it has also been shown that these anisotropic solutions are stable attractors irrespective of the forms of $g(Y)$, provided that they exist in the regime $\Sigma/H \ll 1$. This shows the generality of anisotropic inflation.

If the inflaton couples to a two-form field $B_{\mu\nu}$, the anisotropic hair can also survive during inflation [56]. In such models the sign of g_* is positive, so the scalar power spectrum has a prolate-type anisotropy. The effect of anisotropies appears in a similar way to the scalar and tensor power spectra, i.e., both n_s and r get smaller for larger g_* [59]. The non-linear estimator in the two-form field model is generally smaller than that in the vector model for the same orders of $|g_*|$, so the former is even more likely to satisfy the Planck bounds of non-Gaussianities. In the two-form field model there is no cross correlation between scalar and tensor perturbations [59], while in the vector model the cross correlation does not vanish [55]. Hence these two models can be distinguished observationally. We refer the reader to Refs. [56, 59] for detailed calculations of the inflationary observables.

6. Conclusion

In this review we have constrained a host of inflationary models by using the Planck data combined with other observations. In particular, most single-field inflationary models proposed in the literature belong to a class of the Horndeski theory described by the action (1). We have computed the power spectra of scalar and tensor perturbations in such general theories to confront each model with observations of CMB temperature anisotropies. Since the non-linear estimator f_{NL} of scalar non-Gaussianities in the squeezed limit is much smaller than 1 under the slow-variation approximation, the models based on the Horndeski theory are compatible with the recent Planck bound.

We have applied our general results to concrete models of inflation such as potential-driven slow-roll inflation, k-inflation, Starobinsky inflation, and Higgs inflation with non-minimal/derivative/Galileon couplings. In the potential-driven slow-roll scenario, models such as hybrid inflation ($V(\phi) = \Lambda^4 + m^2\phi^2/2$) and power-law inflation ($V(\phi) = V_0 e^{-\gamma\phi/M_{\text{pl}}}$) are outside the 95 % CL boundary constrained by Planck+WP+BAO+high- ℓ . The monomial potential $V(\phi) = \lambda_n\phi^n/n$ ($n > 0$) is outside the 68 % CL region. In natural inflation with the potential $V(\phi) = V_0[1 + \cos(\phi/f)]$ the symmetry-breaking scale f is constrained as $5.1M_{\text{pl}} < f < 7.9M_{\text{pl}}$ (68 % CL). Very small-field potentials such as $V(\phi) = \Lambda^4(1 - e^{-\phi/M})$ are consistent with the data because of the suppressed tensor-to-scalar ratio.

K-inflation can be tightly constrained by adding the bound on the equilateral non-linear estimator $f_{\text{NL}}^{\text{equil}}$ to those of n_s and r . In the dilatonic ghost condensate model described by the Lagrangian (57), the scalar propagation speed is constrained as $0.034 < c_s < 0.046$ (95 % CL) from the bounds of n_s and r , but, in this parameter range, $|f_{\text{NL}}^{\text{equil}}|$ is too large to be compatible with the Planck data. The same property also holds for the ultraviolet DBI model. In the infrared DBI model the allowed parameter space satisfying all the bounds is constrained to a narrow range.

In Starobinsky inflation the scalar spectral index and the tensor-to-scalar ratio are given by $n_s = 1 - 2/N$ and $r = 12/N^2$ respectively, in which case the model is well within the 68 % CL region. In Higgs inflation, described by the potential $V(\phi) = (\lambda_4/4)(\phi^2 - v^2)^2$ ($v \sim 10^2$ GeV), the presence of non-minimal couplings $-\xi\phi^2 R/2$ with $|\xi| \gg 1$ gives rise to the Einstein-frame potential similar to that in Starobinsky inflation, so that n_s and r are the same in both models as long as quantum corrections to the tree-level Higgs potential are suppressed. It is possible to realize the self coupling λ_4 of the order of 0.1 at the expense of having a large negative non-minimal coupling $\xi \sim -10^4$.

In the presence of the field-derivative coupling to the Einstein tensor or the Galileon self-interactions, the Higgs potential is still outside the 68 % CL region. Although such couplings lead to the decrease of r due to the enhanced friction for the inflaton, these models are not necessarily favored over non-minimally coupled Higgs inflation or Starobinsky inflation because of the tight upper bound on n_s provided by the Planck data.

We have also reviewed anisotropic inflation driven by the presence of a coupling between a vector field and the inflaton. For the coupling (89) an anisotropic hair survives during inflation, so that several observational signatures can be imprinted in CMB. We have derived the anisotropy parameter g_* , appearing in the scalar power spectrum, and have also computed the bispectrum of primordial non-Gaussianities. Under the bound $|g_*| < 0.01$ the non-linear

parameter f_{NL} is smaller than the order of 1, in which case the Planck bound on non-Gaussianities is satisfied. We also note that the anisotropic hair can survive for power-law k -inflation or in the presence of a coupling between a two-form field and the inflaton.

It is expected that future observations of CMB polarization such as LiteBIRD will provide further tight constraints on the amplitude of gravitational waves. We hope that we can approach the best model of inflation in the foreseeable future.

Acknowledgement

The author is supported by the Scientific Research Fund of the JSPS (No. 24540286) and Scientific Research on Innovative Areas (No. 21111006).

References

- [1] A. A. Starobinsky, Phys. Lett. B **91**, 99 (1980).
- [2] D. Kazanas, Astrophys. J. **241** L59 (1980); K. Sato, Mon. Not. R. Astron. Soc. **195**, 467 (1981); Phys. Lett. **99B**, 66 (1981); A. H. Guth, Phys. Rev. D **23**, 347 (1981).
- [3] V. F. Mukhanov and G. V. Chibisov, JETP Lett. **33**, 532 (1981); A. H. Guth and S. Y. Pi, Phys. Rev. Lett. **49** (1982) 1110; S. W. Hawking, Phys. Lett. B **115**, 295 (1982); A. A. Starobinsky, Phys. Lett. B **117** (1982) 175; J. M. Bardeen, P. J. Steinhardt and M. S. Turner, Phys. Rev. D **28**, 679 (1983).
- [4] G. F. Smoot *et al.*, Astrophys. J. **396**, L1 (1992).
- [5] D. N. Spergel *et al.* [WMAP Collaboration], Astrophys. J. Suppl. **148**, 175 (2003).
- [6] P. A. R. Ade *et al.* [Planck Collaboration], arXiv:1303.5076 [astro-ph.CO].
- [7] A. A. Starobinsky, “Nonsingular model of the Universe with the quantum-gravitational de Sitter stage and its observational consequences”, in: Proc. of the 2nd Seminar, “Quantum Gravity” (Moscow, 13-15 Oct. 1981), INR Press, Moscow, 1982, pp. 58-72, M. A. Markov, P. C. West (eds.) Publ. Co., New York, 1984, pp. 103-128); A. Vilenkin, Phys. Rev. D **32**, 2511 (1985); M. B. Mijic, M. S. Morris and W. M. Suen, Phys. Rev. D **34**, 2934 (1986).
- [8] A. D. Linde, Phys. Lett. B **108**, 389 (1982).
- [9] A. Albrecht and P. Steinhardt, Phys. Rev. Lett. **48**, 1220 (1982).
- [10] D. H. Lyth and A. Riotto, Phys. Rept. **314**, 1 (1999).
- [11] A. D. Linde, “Particle Physics and Inflationary Cosmology,” arXiv:hep-th/0503203.
- [12] D. Baumann and L. McAllister, Ann. Rev. Nucl. Part. Sci. **59**, 67 (2009).
- [13] A. Mazumdar and J. Rocher, Phys. Rept. **497**, 85 (2011).
- [14] A. D. Linde, Phys. Lett. B **129** 177 (1983).
- [15] J. E. Lidsey, A. R. Liddle, E. W. Kolb, E. J. Copeland, Rev. Mod. Phys. **69**, 373 (1997).
- [16] A. R. Liddle and D. H. Lyth, *Cosmological inflation and large-scale structure*, Cambridge University Press (2000).
- [17] B. A. Bassett, S. Tsujikawa and D. Wands, Rev. Mod. Phys. **78**, 537 (2006).
- [18] J. Martin, C. Ringeval and V. Vennin, arXiv:1303.3787 [astro-ph.CO].
- [19] P. A. R. Ade *et al.* [Planck Collaboration], arXiv:1303.5082 [astro-ph.CO].
- [20] S. Tsujikawa, J. Ohashi, S. Kuroyanagi and A. De Felice, Phys. Rev. D **88**, 023529 (2013).
- [21] G. Hinshaw *et al.* [WMAP Collaboration], Astrophys. J. Suppl. **208**, 19 (2013).
- [22] F. Beutler *et al.*, Mon. Not. Roy. Astron. Soc. **416**, 3017 (2011); N. Padmanabhan *et al.*, arXiv:1202.0090 [astro-ph.CO]; L. Anderson *et al.*, Mon. Not. Roy. Astron. Soc. **427**, no. 4, 3435 (2013).
- [23] C. L. Reichardt *et al.*, Astrophys. J. **755**, 70 (2012); S. Das *et al.*, arXiv:1301.1037 [astro-ph.CO].
- [24] C. Armendariz-Picon, T. Damour and V. F. Mukhanov, Phys. Lett. B **458**, 209 (1999).
- [25] J. Garriga and V. F. Mukhanov, Phys. Lett. B **458**, 219 (1999).
- [26] D. Seery and J. E. Lidsey, JCAP **0506**, 003 (2005).
- [27] X. Chen, M. x. Huang, S. Kachru and G. Shiu, JCAP **0701**, 002 (2007).
- [28] P. A. R. Ade *et al.* [Planck Collaboration], arXiv:1303.5084 [astro-ph.CO].
- [29] T. Futamase and K. -i. Maeda, Phys. Rev. D **39**, 399 (1989); R. Fakir and W. G. Unruh, Phys. Rev. D **41**, 1783 (1990).
- [30] F. L. Bezrukov and M. Shaposhnikov, Phys. Lett. B **659**, 703 (2008).
- [31] C. Brans and R. H. Dicke, Phys. Rev. **124**, 925 (1961).
- [32] A. Nicolis, R. Rattazzi and E. Trincherini, Phys. Rev. D **79**, 064036 (2009).
- [33] C. Deffayet, G. Esposito-Farese and A. Vikman, Phys. Rev. D **79**, 084003 (2009); C. Deffayet, S. Deser and G. Esposito-Farese, Phys. Rev. D **80**, 064015 (2009).
- [34] T. Kobayashi, M. Yamaguchi and J. 'i. Yokoyama, Phys. Rev. Lett. **105**, 231302 (2010).

-
- [35] C. Burrage, C. de Rham, D. Seery and A. J. Tolley, JCAP **1101**, 014 (2011).
- [36] L. Amendola, Phys. Lett. B **301**, 175 (1993).
- [37] C. Germani and A. Kehagias, Phys. Rev. Lett. **105**, 011302 (2010); C. Germani and A. Kehagias, Phys. Rev. Lett. **106**, 161302 (2011).
- [38] K. Nakayama and F. Takahashi, JCAP **1011**, 009 (2010) [arXiv:1008.2956 [hep-ph]].
- [39] A. De Felice, S. Tsujikawa, J. Elliston and R. Tavakol, JCAP **1108**, 021 (2011).
- [40] G. W. Horndeski, Int. J. Theor. Phys. **10**, 363-384 (1974).
- [41] C. Deffayet, X. Gao, D. A. Steer and G. Zahariade, Phys. Rev. D **84**, 064039 (2011); C. Charmousis, E. J. Copeland, A. Padilla and P. M. Saffin, Phys. Rev. Lett. **108**, 051101 (2012).
- [42] T. Kobayashi, M. Yamaguchi and J. 'i. Yokoyama, Prog. Theor. Phys. **126**, 511 (2011).
- [43] X. Gao and D. A. Steer, JCAP **1112**, 019 (2011).
- [44] A. De Felice and S. Tsujikawa, Phys. Rev. D **84**, 083504 (2011).
- [45] X. Gao, T. Kobayashi, M. Yamaguchi and J. 'i. Yokoyama, Phys. Rev. Lett. **107**, 211301 (2011).
- [46] X. Gao *et al.*, PTEP **2013**, 053E03 (2013).
- [47] S. Mizuno and K. Koyama, Phys. Rev. D **82**, 103518 (2010); A. De Felice and S. Tsujikawa, JCAP **1104**, 029 (2011); T. Kobayashi, M. Yamaguchi and J. 'i. Yokoyama, Phys. Rev. D **83**, 103524 (2011).
- [48] N. E. Groeneboom and H. K. Eriksen, Astrophys. J. **690**, 1807 (2009); D. Hanson and A. Lewis, Phys. Rev. D **80**, 063004 (2009); L. Ackerman, S. M. Carroll and M. B. Wise, Phys. Rev. D **75**, 083502 (2007).
- [49] N. E. Groeneboom, L. Ackerman, I. K. Wehus and H. K. Eriksen, Astrophys. J. **722**, 452 (2010).
- [50] S. R. Ramazanov and G. Rubtsov, arXiv:1311.3272 [astro-ph.CO].
- [51] J. Kim and E. Komatsu, Phys. Rev. D **88**, 101301 (2013).
- [52] M. a. Watanabe, S. Kanno and J. Soda, Phys. Rev. Lett. **102**, 191302 (2009).
- [53] J. Soda, Class. Quant. Grav. **29**, 083001 (2012); A. Maleknejad, M. M. Sheikh-Jabbari and J. Soda, Phys. Rept. **528**, 161 (2013).
- [54] A. E. Gumrukcuoglu, B. Himmetoglu and M. Peloso, Phys. Rev. D **81**, 063528 (2010); T. R. Dulaney and M. I. Gresham, Phys. Rev. D **81**, 103532 (2010).
- [55] M. a. Watanabe, S. Kanno and J. Soda, Prog. Theor. Phys. **123**, 1041 (2010).
- [56] J. Ohashi, J. Soda and S. Tsujikawa, Phys. Rev. D **87**, 083520 (2013).
- [57] N. Bartolo, S. Matarrese, M. Peloso and A. Ricciardone, Phys. Rev. D **87**, 023504 (2013).
- [58] M. Shiraishi, E. Komatsu, M. Peloso and N. Barnaby, JCAP **1305**, 002 (2013).
- [59] J. Ohashi, J. Soda and S. Tsujikawa, JCAP **1312**, 009 (2013).
- [60] A. R. Liddle and S. M. Leach, Phys. Rev. D **68**, 103503 (2003).
- [61] R. L. Arnowitt, S. Deser and C. W. Misner, Phys. Rev. **117**, 1595 (1960).
- [62] J. M. Maldacena, JHEP **0305**, 013 (2003).
- [63] K. Koyama, Class. Quant. Grav. **27**, 124001 (2010).
- [64] V. N. Lukash, Sov. Phys. JETP **52**, 807 (1980).
- [65] J. M. Bardeen, Phys. Rev. D **22**, 1882 (1980).
- [66] H. Kodama and M. Sasaki, Prog. Theor. Phys. Suppl. **78**, 1 (1984); V. F. Mukhanov, H. Feldman and R. Brandenberger, Phys. Rept. **215**, 203 (1992); K. A. Malik and D. Wands, Phys. Rept. **475**, 1 (2009).
- [67] E. Komatsu and D. N. Spergel, Phys. Rev. **D63**, 063002 (2001).
- [68] N. Bartolo, S. Matarrese, A. Riotto, Phys. Rev. **D65**, 103505 (2002); N. Bartolo, E. Komatsu, S. Matarrese and A. Riotto, Phys. Rept. **402**, 103 (2004).
- [69] A. De Felice and S. Tsujikawa, JCAP **1303**, 030 (2013).
- [70] P. Creminelli and M. Zaldarriaga, JCAP **0410**, 006 (2004).
- [71] F. Arroja, A. E. Romano and M. Sasaki, Phys. Rev. D **84**, 123503 (2011); P. Adshead, C. Dvorkin, W. Hu and E. A. Lim, Phys. Rev. D **85**, 023531 (2012); X. Chen, H. Firouzjahi, M. H. Namjoo and M. Sasaki, Europhys. Lett. **102**, 59001 (2013).
- [72] G. Mangano *et al.*, Nucl. Phys. B **729**, 221 (2005).
- [73] K. Ichikawa and T. Takahashi, Phys. Rev. D **73**, 063528 (2006).
- [74] L. Randall and R. Sundrum, Phys. Rev. Lett. **83**, 4690 (1999); R. Maartens, D. Wands, B. A. Bassett and I. Heard, Phys. Rev. D **62**, 041301 (2000).
- [75] R. Brandenberger and P. -M. Ho, Phys. Rev. D **66**, 023517 (2002).
- [76] G. Calcagni, S. Kuroyanagi, J. Ohashi and S. Tsujikawa, JCAP **1403**, 052 (2014).
- [77] L. McAllister, E. Silverstein and A. Westphal, Phys. Rev. D **82**, 046003 (2010).
- [78] E. Silverstein and A. Westphal, Phys. Rev. D **78**, 106003 (2008).
- [79] K. Freese, J. A. Frieman and A. V. Olinto, Phys. Rev. Lett. **65**, 3233 (1990); F. C. Adams, J. R. Bond, K. Freese, J. A. Frieman and A. V. Olinto, Phys. Rev. D **47**, 426 (1993).
- [80] A. D. Linde, Phys. Rev. D **49**, 748 (1994).
- [81] G. R. Dvali, Q. Shafi and R. K. Schaefer, Phys. Rev. Lett. **73**, 1886 (1994).
- [82] D. H. Lyth, Phys. Rev. Lett. **78**, 1861 (1997).
- [83] D. H. Lyth, Lect. Notes Phys. **738**, 81 (2008) [hep-th/0702128].

-
- [84] G. R. Dvali and S. H. H. Tye, Phys. Lett. B **450**, 72 (1999).
- [85] J. P. Conlon and F. Quevedo, JHEP **0601**, 146 (2006).
- [86] S. Kachru *et al.*, JCAP **0310**, 013 (2003); J. J. Blanco-Pillado *et al.*, JHEP **0609**, 002 (2006); D. Baumann, A. Dymarsky, I. R. Klebanov and L. McAllister, JCAP **0801**, 024 (2008); S. Panda, M. Sami and S. Tsujikawa, Phys. Rev. D **76**, 103512 (2007).
- [87] F. Piazza and S. Tsujikawa, JCAP **0407**, 004 (2004).
- [88] N. Arkani-Hamed, H. C. Cheng, M. A. Luty and S. Mukohyama, JHEP **0405**, 074 (2004); N. Arkani-Hamed, P. Creminelli, S. Mukohyama and M. Zaldarriaga, JCAP **0404**, 001 (2004).
- [89] E. Silverstein and D. Tong, Phys. Rev. D **70**, 103505 (2004).
- [90] M. Alishahiha, E. Silverstein and D. Tong, Phys. Rev. D **70**, 123505 (2004).
- [91] D. Baumann and L. McAllister, Phys. Rev. D **75**, 123508 (2007); J. E. Lidsey and I. Huston, JCAP **0707**, 002 (2007).
- [92] X. Chen, Phys. Rev. D **71**, 063506 (2005).
- [93] J. Ohashi and S. Tsujikawa, Phys. Rev. D **83**, 103522 (2011).
- [94] J. O'Hanlon, Phys. Rev. Lett. **29**, 137 (1972); T. Chiba, Phys. Lett. B **575**, 1 (2003).
- [95] K. -i. Maeda, Phys. Rev. D **39**, 3159 (1989).
- [96] N. Makino and M. Sasaki, Prog. Theor. Phys. **86**, 103 (1991); D. I. Kaiser, Phys. Rev. D **52**, 4295 (1995); A. De Felice and S. Tsujikawa, Living Rev. Rel. **13**, 3 (2010).
- [97] L. A. Kofman, V. F. Mukhanov and D. Y. Pogosian, Sov. Phys. JETP **66**, 433 (1987); J. -c. Hwang and H. Noh, Phys. Lett. B **506**, 13 (2001).
- [98] S. V. Ketov and A. A. Starobinsky, Phys. Rev. D **83**, 063512 (2011); S. V. Ketov and S. Tsujikawa, Phys. Rev. D **86**, 023529 (2012); J. Ellis, D. V. Nanopoulos and K. A. Olive, Phys. Rev. Lett. **111**, 111301 (2013); Y. Watanabe and J. 'i. Yokoyama, Phys. Rev. D **87**, 103524 (2013); R. Kallosh and A. Linde, JCAP **1306**, 028 (2013); R. Kallosh and A. Linde, JCAP **1307**, 002 (2013); F. Farakos, A. Kehagias and A. Riotto, Nucl. Phys. B **876**, 187 (2013); W. Buchmuller, V. Domcke and K. Kamada, Phys. Lett. B **726**, 467 (2013); F. Briscece, A. Marciano, L. Modesto and E. N. Saridakis, Phys. Rev. D **87**, 083507 (2013); F. Briscece, L. Modesto and S. Tsujikawa, Phys. Rev. D **89**, 024029 (2014).
- [99] E. Komatsu and T. Futamase, Phys. Rev. D **59**, 064029 (1999); S. Tsujikawa and B. Gumjudpai, Phys. Rev. D **69**, 123523 (2004).
- [100] C. Germani, L. Martucci and P. Moyassari, Phys. Rev. D **85**, 103501 (2012).
- [101] A. Berera, Phys. Rev. Lett. **75**, 3218 (1995); S. Bartrum *et al.*, arXiv:1307.5868 [hep-ph].
- [102] C. Germani and Y. Watanabe, JCAP **1107**, 031 (2011).
- [103] S. Tsujikawa, Phys. Rev. D **85**, 083518 (2012).
- [104] K. Kamada, T. Kobayashi, M. Yamaguchi and J. 'i. Yokoyama, Phys. Rev. D **83**, 083515 (2011).
- [105] J. Ohashi and S. Tsujikawa, JCAP **1210**, 035 (2012).
- [106] S. Tsujikawa, Phys. Rev. D **73**, 103504 (2006); L. Amendola, M. Quartin, S. Tsujikawa and I. Waga, Phys. Rev. D **74**, 023525 (2006).
- [107] J. Ohashi, J. Soda and S. Tsujikawa, Phys. Rev. D **88**, 103517 (2013).